We would like to thank Anonymous Referee #1 for his evaluations and positive feedback. Comments (mostly linguistic) that were provided in the attached annotated version of the manuscript were incorporated in the revised text.

Below we list answers to the specific comments:

(1) At the beginning of the "3.2 Processing" section, the paragraph beginning at line 35 mentions "sediments". Sediment usually refers to unconsolidated material. Do the authors mean "sedimentary rock". Moreover, I do not know what the authors mean by "keep the original sweep bandwidth in the sediments". This makes no sense to me with any interpretation of these words that I can think of. A rewrite of this sentence is warranted.

We changed "sediments" into "sedimentary cover". We also rewrote the sentence regarding the original ION processing, now it reads: "preserve the original sweep bandwidth in the sedimentary cover"

(2) In the "4 Results" section, beginning at line 5, amplitude decay curves are described. Were these calculated before or after AGC. The answer to this is likely to have implications for the interpretation of these curves.

Yes, indeed those decay curves were calculated after the AGC (which we overlooked somehow initially). Therefore, in this case, we cannot use them to properly decipher the signal penetration limits. However, we can still track relative amplitude changes and this is mostly why we use those plots – in our opinion, they were helpful to e.g. determine the Moho depth.

(3) The line numbering the convention that starts over ever 45 lines is not useful.

This is the default numbering scheme used by Copernicus in their template.

On behalf of the authors,

M. Mężyk

We would like to thank Anonymous Referee #2 for his evaluations and positive feedback.

Below we list answers to the general and specific comments:

The rational for some parts of the interpretation requires clarification, for example the interpretation of the anorthosite intrusions in transparent regions of the crust. Nonreflective zones occur in many areas, but can only be reasonably, and speculatively, inferred to be intrusions where underlying reflections are present, demonstrating good signal penetration into the deeper crust. Why isn't the transparent crust at 6-24 km between CDP 5000 and 6000 on line 1200 interpreted to be a pluton? Consistency in the interpretation is necessary.

Now, we added some explanation, as well as brought the magnetic anomaly plots on top of the interpretation figures. The revised text reads: "The interpreted shapes of the AMCG bodies in Figures 7-9 are only tentative and rely on coincidence of three evidences: (1) presence of mostly transparent crust in seismic sections, (2) occurrence of the AMCG suite outcrops at the top of the basement (after Krzemińska et al., 2017), and (3) concurrence of magnetic highs (Figs 3, 7-9) due to elevated magnetic susceptibility of the AMCG rocks"

What are the black lines on the interpreted seismic sections intended to show? Are they intended to indicate representative reflection fabrics or shear zones or something else; the first is a characterization of the data to assist the reader, the second is an interpretation, which requires more explanation, even if only in general terms.

Black lines shown in the interpreted figures indeed indicate representative reflection fabric, shear zones, truncations, etc. Our interpretation of the data is kept to minimum. Probably the most subjective features are the inferred positions of the AMCG suites. In the revised text we added the following sentence: "Black lines in Figs. 7-9 delineate representative reflection fabrics and shear zones, which we infer from the data."

How do you define the lower crust mentioned on page 6, lines 10-12, i.e. it's top as Moho is already inferred?

Similarly to Moho, we used WARR-derived top of the lower crust as a guideline. Then, with such a proxy of the lower crust depth, we checked the change in reflectivity patterns between middle/lower crustal level. It led us to the conclusion about the reduced thickness of the lower crust as compared with the WARR model.

When discussing features on the seismic sections, it would greatly help the reader if they were identified on the figure by a label that was then referenced in the text.

We added now labels (S, C', T) to interpretation figures and cross-reference them in the text.

The inference of S-C' fabrics is an interesting result, but needs to be clearly demonstrated, because I couldn't really see this in the data. I suggest adding a cartoon-like figure to explain what structure you are inferring from the data, and a couple of labels on the seismic to explain where these features are seen. What do you mean by non-coaxial flow? Be clear on direction relative to strike of orogeny.

We added a new figure (Fig. 10) with a cartoon showing S-C' structure formation. Non-coaxial flow is a deformation in which the lines parallel to the principal strain axes have rotated away from their initial positions (as in simple shear).

Equations (1) to (3) are not really necessary as most specialists are familiar with them, but they could be retained, but in this case the assumptions should be stated, e.g. linear sweep. All sweep parameters

should be included in the text: start and end frequencies, type of sweep, e.g. linear upsweep, start and end tapers etc.

We kept the equations for completeness. All sweep parameters are listed as well.

The number of figures could be reduced. Figure 3 is not really necessary unless the authors are going to interpret plutons from the magnetic fabric shown or to clearly use the figure for some specific aspect of the interpretation.

In fact, we increased number of figures in the revised version. We prefer to keep Fig. 3, as it's showing magnetic highs related to plutons. Now, those AMCG complexes are indicated in Fig. 3. We also added magnetic anomaly plots above the interpreted sections to support interpretation of the AMCG bodies (see the first comment). Because of this, 2 figures with interpretation had to be split into 3 figures (Fig. 7-9).

It is useful to see the comparison of displays in Figure 4, but I think Figure 5 could be omitted, especially if the number of black lines, many of which are not clearly justified, is reduced in the interpreted sections.

We prefer to keep "clean" uninterpreted sections in Fig. 4-5 and then their interpreted counterparts in the revised Fig. 7-9

The frequency decay in the lower panel in Figure 6 does not contribute much and can also be removed, but the refraction Moho, or its range over these parts of the lines, should be indicated in the upper panel.

We removed the frequency-decay curves and added the averaged WARR Moho location.

Minor comments, questions and suggested edits:

Majority of those, mostly editorial, corrections were implemented in the revised manuscript (see the manuscript in the track-changes mode). We list of all the suggestions for completeness, but only those requiring more detailed answer are commented below.

Title suggestion: Imaging the East European Craton margin in Northern Poland using extended correlation processing of regional seismic reflection profiles

We changed it accordingly

P1,L8: remove both "the"
P1,L11: 3-layer cratonic crust
P1,L15: which we primarily associate with Paleoproterozoic crust formed during
P1,L16: and are similar to those observed…
P1,L18: What is direction of crustal flow: orogeny normal? Be specific.
P1,L19: Didn't you indicate shortening in the text, so why extension here? Not clear.
P1,L22: of thickened crust
P2,L9: by refraction
P2,L10: define LT. They portray relatively
P2,L13: 1980s. Give years acquired
P2,L17: aimed to provide
P2,L19: data has already
P2,L20: These seismic profiles have been used as
P2,L20: a new interpretation

P2,L22: deformation extends much
P2,L23: showed that these… study deep
P2,L27: apply extended
P2,L28: Precambrian crust
P2,L29: cover, previous inferences were based mostly on
P2,L30: (K..,2017), but with these new seismic reflection data it is now possible
P2,L31: these new data
P2,L32: to that observed
P2,L33: remove ? … of Mesoproterozoic magmatism
P3,L1: Can you indicate the known extent of the Svecofennian orogeny in Figure 1? Is it defined by the coloured terranes in Figure 1. If so, please state explicitly.
Made clear in the revised caption.
P3,L2: with a 1.83-1.84 Ga
P3,L6: has been recognized
P3,L7: during Rodinia breakup
P3,L8: has been recognized
P3,L98: by Caledonian
P3,L14: by PolandSPAN
P3,L23: are clearly visible
P3,L24: Refer to labels on Fig.3 to indicate intrusions
We overlaid location of the AMCG intrusions shown in Fig. 2 in Fig. 3 now.
P3,L27: employed acquisition
P3,L31: recorded with
P3,L35: structure with a processing sequence optimized to preserve the
P3,L39: that by using
P3,L40: the PolandSPAN data could be
P4,L2: upsweep. This is important!
P4,L5: means that the reference signal we correlate with the recorded data was truncated during the correlation process, preserving the full bandwidth for the original record length, but losing bandwidth at later times.
P4,L30: Define Vrms
P4,L32: Why is DMO ”vital”? DMO applies very little correction at late times, so is the effect due to the suppression of steeply dipping noise, i.e. similar to an F-K filter. How was DMO applied? F-K in common offset or Kirchhoff implementation? Are these crooked lines, which will affect results of algorithm: F-K not tur 3-D DMO, but Kirchhoff may be.
We agree that the sensitivity of DMO at later times is low. Anyway, in our case there was a clear uplift in the stacks after DMO observed – both in reflector continuity and overall signal-to-noise improvement. We run Kirchhoff DMO on offset planes. The geometry of the profiles are smoothly-varying, with shots kept within 200 m of the receiver line, so they are not considered as typical ‘crooked lines’
P5,L9: yields curves
P5,L10-13: Not clear to me exactly how the frequency decay curves were computed, e.g. what “amplitude values”. Needs to be reworded. However, since I suggested that these displays be removed, this section could be omitted with corresponding edits elsewhere.
In fact, in the revised version we removed frequency-decay curves.
P5,L20: Cite figures here
P5,L21: From exactly what feature are you tracking the lower crust-mantle transition? Downward termination of reflectivity, but note there are coherent events in the mantle, which could be noise, so you need to exclude these, and explain how/why.
We believe that this can be deduced from the text between lines 21-33 on page 5 in the original manuscript, where we also mention sub-Moho reflectivity vs migration artifacts/noise. However, we

modified the opening sentence in the revised manuscript: "The transition between the lower crust and the uppermost mantle is often trackable (as a change in a generally reflective crust vs transparent mantle or as a band of stronger reflectivity at the expected Moho depth)".
P5,L24: would flatten out at 20 km
P5,L25: In contrast to the poorly
P5,L27: and extends for
P5,L28: Moho can also be inferred from both amplitude… which we present in
P5,L29: time where the curves do not decay further
P5,L31: some reflections might continue into the upper mantle, such as events visible on line 5600
P5,L33: the one on line 5600
P5,L35: Poland show a much more... crust compared with
P5,L36: which is a result of the different methodologies employed. DELETE TO. However, as discussed
P6,L2: defined as the base of bands of intermittent reflections dividing
P6,L10-12: How are you defining the lower crust using the reflection data? Explain.
Already explained in the 'general comments'. We added additional explanation in the revised manuscript: "The depth to lower crust was inferred using WARR data and the change in the reflectivity patterns observed between the middle/lower crustal depths."
P6,L17: Label these features on figures. How are they inferred from the seismic reflections or gaps in seismic reflectivity.
Explanation and labels added.
P6,L25: Use label to indicate position in Figure 7.
P6,L27-39: This can be explained
P7,L2: 2005) due to the structural record
P7,L10: of AMCG magmatism
P7,L13: How related to lower crustal delamination? Please clarify.
This part was reworded to "Increased mantle reflectivity in the vicinity of the AMCG bodies may signify fragments of delaminated lower crustal material".
P7,L15: of a lower/middle
P7,L38-39: with Caledonian deformation… represent a Proterozoic
P8,L4: with Paleoproterozoic crustal formation… Orogeny, and which are similar to those observed
P8,L13: basement may be linked

Figure 1: Darken coastline to make location of terranes clearer with respect to NE Europe.
Changed accordingly
Figure 4,5,7: Distance scale is too small to be legible. Depth annotation does need to be so frequent, perhaps every 5 km?
Changed accordingly

On behalf of the authors,

M. Mężyk

Imaging the East European Craton margin in ~~Northern~~northern Poland using extended-correlation processing ~~applied to~~of regional seismic reflection ~~seismic~~ profiles

Miłosz Mężyk[1], Michał Malinowski[1], Stanisław Mazur[2]

[1]Institute of Geophysics Polish Academy of Sciences, Warsaw, 01-452, Poland
[2]Institute of Geological Sciences Polish Academy of Sciences, 00-818, Warsaw, Poland

Correspondence to: Miłosz Mężyk (mmezyk@igf.edu.pl)

Abstract. In NE Poland, ~~the~~ Eastern European Craton (EEC) crust of ~~the~~ Fennoscandian affinity is concealed under a Phanerozoic platform cover and penetrated by the sparse deep research wells. Most of the inferences regarding its structure rely on geophysical data. Until recently, this area was covered only by the refraction/wide-angle reflection (WARR) profiles, which show a relatively simple crustal structure with a typical 3-layer cratonic ~~3 layer~~ crust. ION Geophysical PolandSPAN™ regional seismic program data, acquired over the marginal part of the EEC in Poland, offered a unique opportunity to derive a detailed image of the deeper crust. Here, we apply extended correlation processing to a subset (~950 km) of the PolandSPAN™ dataset located in NE Poland, which enabled us to extend the nominal record length of the acquired data from 12 to 22 s (~60 km depth). Our new processing revealed reflectivity patterns, ~~that~~which we primarily associate with the Paleoproterozoic crust ~~formation~~formed during the Svekofennian (Svekobaltic) orogeny and ~~which~~ are similar to ~~what was~~those observed along the BABEL and FIRE profiles in the Baltic Sea and Finland, respectively. We propose a mid- to lower-crustal, orogeny-normal lateral flow model to explain the occurrence of two sets of structures that can be collectively interpreted as kilometre-scale S-C' shear zones. The structures define a penetrative deformation fabric invoking ductile extension of hot orogenic crust~~.~~ in a convergent setting. Localized reactivation of these structures provided conduits for subsequent emplacement of gabbroic magma that produced a Mesoproterozoic anorthosite-mangerite-charnockite-granite (AMCG) suite in NE Poland. Delamination of ~~overthickened~~thickened orogenic lithosphere may have accounted for ~~magnatic~~magmatic underplating and fractionation into the AMCG plutons. We also found sub-Moho dipping mantle reflectivity, which we tentatively explain as a signature of the crustal accretion during the Svekofennian orogeny. Later tectonic phases (e.g. Ediacaran rifting, Caledonian orogeny) did not leave a clear signature in the deeper crust, however, some of the subhorizontal reflectors below the basement, observed in the vicinity of the AMCG Mazury complex, can be alternatively linked with lower Carboniferous magmatism.

1 Introduction

The Precambrian East European Craton (EEC) is composed of three major crustal blocks: Fennoscandia, Sarmatia and Wolgo-Uralia (Gorbatschev and Bogdanova, 1993). Fennoscandia was formed in the Paleoproterozoic during the Svecofennian orogeny (see e.g., Lahtinen et al., 2009). Its crust was imaged by several deep reflection profiles mostly offshore (Baltic Sea) (Abramovitz et al., 1997; BABEL Working Group, 1993; Korja and Heikkinen, 2005; Meissner and Krawczyk, 1999) with a notable exception of the FIRE project onshore Finland (Kukkonen and Lahtinen, 2006; Torvela et al., 2013). In NE Poland, the Fennoscandian crust is concealed under a Phanerozoic platform cover and is penetrated by the sparse deep research wells ~~(see~~. See Krzemińska et al~~.,~~ . (2017) for a recent summary~~).~~. Therefore, most of the inferences regarding its structure rely on the geophysical data. Until recently, this area was covered only by ~~the~~ refraction/wide-angle reflection (WARR) profiles from the POLONAISE'97 project (P2, P3, P4, P5 profile, Czuba et al., 2002; Grad et al., 2003; Janik et al., 2002; Środa et al., 1999) and legacy ~~LT~~ transects (LT-7 profile, Guterch et al., 1994). They ~~portrait~~portray relatively simple crustal structure with typical cratonic 3-layer crust (Grad et al., 2010). Experimental deep reflection seismic profile GB1 shot ~~in the 80s~~between 1987-88 revealed complex reflectivity patterns in the deeper crust of the Pomerania region (Dziewinska and Tarkowski, 2016), but the low quality of the seismic data precludes any definite interpretation. ~~It was only recently, that~~Recently this area was covered by the deep reflection seismic profiles of the ION Geophysical PolandSPAN™ project. In 2012, ten PolandSPAN™ profiles (with a total length of 2200 km) were acquired in Poland over the marginal part of the EEC, east of the Teisseyre-Tornquist Zone (TTZ). This large, regional seismic program aimed ~~at providing~~to provide a better understanding of the sedimentary history, tectonic architecture and basement structure of the lower Paleozoic shale basins (Krzywiec et al., 2013). Because of its regional character and unprecedented imaging quality, PolandSPAN™ data has already revolutionized several aspects of the regional geology of Poland. ~~They were~~These seismic profiles have been used as constraints for potential-field modelling that led to ~~the~~a new interpretation of the TTZ (Mazur et al., 2015, 2016b) and Polish Caledonides (Mazur et al., 2016a). In SE Poland, interpretation of the PolandSPAN™ profiles proved that the Variscan ~~deformations are extending~~deformation extends much further to the east than previously assumed (Krzywiec et al., 2017a, 2017b). Malinowski (2016) ~~proved~~showed that these data can be effectively used to study ~~the~~ deep crustal structure by employing the extended correlation method of Okaya and Jarchow (1989), showing, e.g. presence of the reflective lower crust underlying the EEC in SE Poland, previously imaged by the POLCRUST-01 profile (Malinowski et al., 2013, 2015).

Here, we apply ~~the~~ extended correlation processing to a subset of the PolandSPAN™ data located in NE Poland: 3 dip (5400, 5500, 5600) and 2 strike profiles (1100, 1200) with a total length of ~950 km. Since ~~the~~ Precambrian crust in Poland is concealed beneath a Phanerozoic platform cover ~~and all the~~, previous inferences were based mostly on the sparse deep research wells available (Krzemińska et al., 2017), ~~it is for the first time~~but with these new seismic reflection data it is now possible to shed a light on the characteristics of the deeper EEC crust in NE Poland. The key questions we would like to address using ~~this~~these new data are as follows: (i) is the image of the Svecofennian orogen in NE Poland similar to ~~what is~~that observed further north in Fennoscandia, e.g. in the Bothnian Bay (Korja and Heikkinen, 2005) and onshore Finland (Torvela et al., 2013)?, (ii) do we see a crustal expression of the Mesoproterozoic magmatism?, (iii) are the later tectonic events (like Ediacaran rifting of Rodinia or Caledonian tectonics) also recognizable in the crustal reflectivity patterns? We start with the geological background, then we summarize the processing steps focused on enhancing deeper reflectivity and finally we present the new results and integrate them with the existing geological observations to provide some preliminary interpretation of the crustal structure in NE Poland.

2 Geological background

The study area is located in NE Poland at the western margin of the EEC/Fennoscandia (Fig. 1). Its core was formed during the Paleoproterozoic Svecofennian orogeny, which involved accretion of several microcontinents and island arcs (Lahtinen et al., 2009). Lahtinen et al. (2009) distinguish a separate phase of the Svecofennian accretion, called the Svecobaltic orogeny (1.83-1.8 Ga). In the cross-Baltic correlations by Bogdanova et al. (2015), the area of NE Poland belongs to a microcontinent called Amberland (Fig. 1) with ~~the~~a 1.83-1.84 Ga accretion age. Subsequently, the Paleoproterozoic crust was influenced by the Mesoproterozoic (1.54-1.45 Ga) anorogenic magmatic activity producing anorthosite-mangerite-charnockite-granite (AMCG) complexes in a ~600 km long zone stretching from Belarus, through Lithuania, NE Poland and southern Baltic Sea (Dörr et al., 2002; Skridlaite et al., 2003; Krzemińska et al., 2017). No signature of the Svekonorwegian orogeny (1.14-0.9 Ga) affecting the western rim of Fennoscandia (Bogdanova et al., 2008) was recognized in our study area. Ediacaran rifting during ~~the~~ Rodinia break-up (e.g., Johansson, 2009) eventually led to the formation of a passive margin of Baltica in the early Cambrian. No magmatic activity related to this stage of the EEC margin development ~~was~~has been recognized in NE Poland. The western part of the study area was also affected by ~~the~~ Caledonian tectonics. An extensive flexural basin, named the Baltic Basin, was developed in the Silurian in front of the Caledonian orogen. The basin focused deposition of a fine-grained siliciclastic succession up to 4000 m thick that gradually thins out to the east and constitutes most of the Phanerozoic platform cover of the EEC. The western part of the Baltic Basin was intensely folded to form the Pomeranian Caledonides. The concept of Pomeranian Caledonides was initially based on the analysis of the deep research wells (Dadlez et al., 1994), but it was recently confirmed by ~~the~~ PolandSPAN™ line 5600, which was interpreted to image the frontal thrust of the deformed Upper Ordovician and Silurian sedimentary succession with the undeformed lower Paleozoic sediments of the Baltic Basin (Mazur et al., 2016a). The youngest magmatic episode affecting the EEC crust included lower Carboniferous (354-338 Ma) alkali magmatism with several syenite intrusions (Fig. 2; e.g., Krzemińska et al., 2017), coeval with the dolerite sills intruding Silurian sediments offshore Lithuania (Motuza et al., 2015). According to the revised lithostratigraphy (Krzemińska et al., 2017), crystalline basement units of the study area can be further subdivided into the Dobrzyń Domain (DD), Mazury Complex (MC) and Pomerania-Blekinge Belt (PBB) (Fig. 2). The DD (1.82-1.76 Ga) basement comprises synorogenic granites and supracrustal paragneisses. The PBB (1.79-1.74 Ga) basement includes synorogenic granodiorites, quartz monzonites and granites, whereas the MC (1.54-1.49 Ga) is composed of the anorogenic AMCG association: quartz monzonites, charnockitoids, diorites and monzogabbros. Their occurrences are ~~well~~ clearly visible in the magnetic anomaly map as magnetic highs (Fig. 3).

3 Data and methods

3.1 Acquisition

The PolandSPAN™ project employed ~~high-end~~ acquisition parameters that were primarily optimized to provide a continuous image of the lower Paleozoic shale basins. Data were acquired with a 25 m receiver/shot spacing and 960-channel symmetric spread (max. offset of 12 km), providing nominal fold of 480 with a CDP spacing of 12.5 m. The source array consisted of four INOVA AHV-IV Commander (62,000 lb. peak force) Vibroseis trucks. A custom broadband (2-150 Hz) 16-s long (τ_{sweep}) ~~sweep~~upsweep was used. In the field, uncorrelated data (28 s of listen time, τ_{record}) were recorded ~~alongside~~ with auxiliary data containing measurements of weighted-sum ground force (F_{WS}), an estimate of the vibrator ground force (F_g) (Ziolkowski, 2010) for each vibrator in the array.

3.2 Processing

ION Geophysical original time and depth imaging were focused on the sedimentary cover structure~~. Processing~~ with a processing sequence ~~was~~ optimized to ~~keep~~preserve the original sweep bandwidth in the ~~sediments~~sedimentary cover. Reflection tomography was used to build the velocity model for pre-stack depth migration (PSDM) in the ~~sediments~~sedimentary section, while below the basement, WARR-derived velocities were used. The nominal record length of 12 s enabled imaging down to the lower crust on average. Malinowski and Brettwood (2013) and Malinowski (2016) provided a proof-of-concept that by using the extended correlation method of Okaya and Jarchow (1989), PolandSPAN™ data ~~can~~could be extended to greater times (~20 s). ~~It was~~Malinowski (2016) also demonstrated, that despite relatively short (16 s vs 45-60 s long sweeps used during the POLCRUST-01 acquisition, Malinowski et al., 2013) and broadband (2-150 Hz as opposed to 6-64 Hz) ~~sweep~~upsweep, reliable imaging of the deeper structures (including the Moho) can be obtained.

Therefore, the first step in our reprocessing was the application of the self-truncating extended correlation, which increased the nominal record length $t_{profile}$ from 12 s to 22 s. "Self-truncating" means that the reference signal we correlate with ~~truncates on its own~~the recorded data was truncated during the correlation process, preserving the full ~~frequency band~~ bandwidth for the original record length, but losing bandwidth at ~~the extended time.~~later times. Given the acquisition parameters of the PolandSPAN™ survey, a maximum frequency f_{max} was limited to 57.5 Hz at 22 s of extended time. It can be derived using the following formulas of Okaya and Jarchow (1989~~):~~), assuming linear upsweep:

$$\tau_{record} = \tau_{sweep} + \tau_{listen} \tag{1}$$

$$t_{profile} = \tau_{record} - \tau_{sweep} \tag{2}$$

$$f_{max}(t) = f_1 \qquad 0 \le t \le t_{profile} \tag{3}$$

$$f_{max}(t) = f_1 - \frac{f_1 - f_0}{\tau_{sweep}}(t - t_{profile}) \qquad t_{profile} \le t \le \tau_{record}$$

In the case of Vibroseis acquisition, data are usually correlated with the theoretical (pilot) sweep. As mentioned above, for the PolandSPAN™ data, we have the ground-force estimates for every Vibroseis point (VP) location. When Malinowski (2016) compared stacks of the data correlated with both pilot sweep and ground force estimate averaged over all VPs, he found out that substituting one for another in the correlation process, did not contribute to a significant change in the final stack quality. However, in this study, we prefer to correlate raw data with a ground force averaged for every VP, since ~~it is more realistic to use~~ spatially-varying ground-force estimates (which should compensate for variable baseplate coupling~~), rather~~) are more realistic than a simple theoretical signal.

After the re-correlation process, we started the basic processing sequence, which was focused on the mid- to lower crust and the upper mantle depths. For quality control purposes, several stacked sections for each line were produced at various stages and thoroughly assessed in terms of how processing methods and their parameters affected the seismic signal. Following this routine, the most effective processing sequence and parameter configuration were determined. The processing is summarized in Table 1.

We put a lot of effort into estimating the refraction static corrections, ~~as~~because we decided not to use the contractor's solution. Towards this end, we employed an in-house Neural Network based algorithm (Mezyk and Malinowski, 2018) for picking first breaks. Both elevation statics and refraction statics were applied here, using a datum elevation of 400 m and a replacement velocity of 2250 m/s (same as for original processing). Initially, we processed the data with a relative-amplitude preservation, however, it turned out that qualitatively better results for the deeper crust were obtained with a pre-stack AGC scaling (5 s window). We used ION Geophysical pre-stack time migration (PSTM) root-mean-square (Vrms) velocity models for the NMO/DMO corrections. Mild coherency filtering was applied pre-stack (only FX deconvolution). Dip moveout corrections (DMO) appeared to be ~~vital.~~an essential step. We used Kirchhoff integral-based DMO algorithm on the

common-offset planes. It brought improvements into the sections, by strengthening the continuity of reflectors and correcting for conflicting dips. In general, migrating the DMO-corrected stacked sections provided a clearer image with increased reflection consistency both in the vertical and horizontal direction. After the DMO-stack, signal coherency was substantially increased with a post-stack linear dip filtering. ~~It required careful~~Careful tuning of the parameters was required not to create artificial events. Dip-filtered stacks were subsequently migrated. We tested the line-segment migration code (Calvert, 2004), but because of the generally noisier appearance of such migrated sections, we prefer to use simple F-K (Stolt) migration. Finally, depth conversion was carried out. Velocity models for depth conversion were merged from the PSDM velocity models provided by ION Geophysical for the section above the basement and the compilation of the crustal velocity model for Poland derived from WARR data (~~Grad et al. 2016)~~Grad et al., 2016) for the deeper section below the basement.

4 Results

Final migrated, depth-converted sections, presented in Figures 4 and 5, formed the basis for defining the structural relationships and reflector orientations. The reprocessed profiles illustrate a variety of crustal reflectivity patterns, reflection Moho and dipping mantle reflections. In order to facilitate interpretation, the amplitude envelope is computed from the final stacks, smoothed, and displayed as a colour background.

Signal-penetration depth was estimated from the amplitude ~~and average frequency~~ decay curves (Fig. 6), extracted from the final stacked sections, following Barnes (1994). In order to detect amplitude variability along the profiles, each seismic section is divided into two parts within which the corresponding decay curves are calculated. Amplitude-decay curves represent the root-mean-squared (RMS) amplitude generated using a 200-ms long sliding window that yields ~~the curves not too smooth nor overly spiky. In order to derive frequency decay curves, first, the amplitude spectra were computed for each CDP trace in 200 ms long windows. Next, the weighted average was applied individually to all of the spectra in the frequency range of 10-20 Hz, where weights were defined by amplitude values. The average frequency in windows was subsequently averaged again over the CDP range, which produced a single curve for each half of the profile.~~curves not too smooth nor overly spiky.

Analysis of the reprocessed seismic sections show that, in general, reflectivity of the crust is not stationary, and its intensity may vary from high (e.g. L1200 at 3000-6000 CDP) to low (e.g. L5400 at 3500-5000 CDP), or even can be characterized as acoustically transparent (e.g. L5400 at 1500-3500 CDP), indicating gradual transition from crustal to mantle rocks. Observed intracrustal reflections are mostly discontinuous, but not chaotic. They form patterns that can be either subhorizontal (e.g. L5400 at ~8 km & 5000-10000 CDP) or gently dipping at an angle not exceeding 20 degrees (e.g., L5600 at 12-22 km & 7000-11000 CDP). The presence of abnormally strong reflectivity zones can also be marked, especially in a depth range of 20 to 36 km in the area where lines 5400 and 1200 are crossing~~.~~ (Fig. 4-5). The transition between the lower crust and the uppermost mantle is often trackable~~,~~ (as a change in a generally reflective crust vs transparent mantle or as a band of stronger reflectivity at the expected Moho depth), undulating slightly between 36-42 km, yet in some parts of the stacked sections, the signal penetration is insufficient to image Moho. It is clearly visible in the case of line 5400, where the amplitude decay curves calculated for the SW and NE part are substantially different in terms of the reflectivity strength. Without averaging over thousands of CDPs, the decay amplitudes would ~~die~~ flatten out ~~by reaching~~at 20 km for the transparent CDP interval between 1500 and 3500. In ~~contrary~~contrast to the poorly defined Moho in this part of line 5400, a very sharp boundary is observed along line 5600 and 1200, in a CDP range of 3000-6000 and 1-2500, respectively. The stacked section for line 5400 shows the evidence of a small symmetrical Moho uplift, that emerges around CDP 6000 and ~~spans~~extends for ~90 km in the NE direction. The Moho ~~is~~can also ~~apparent on both~~be inferred from the amplitude ~~and frequency~~ decay curves (which we ~~tend to~~ present in the time domain as originally calculated) as a change in a decay rate at 13±1 s of two-way time~~,~~ where

the curves ~~cease to~~do not decay~~. It~~ further. This time corresponds roughly to a depth of 40 km, a level characterized by sudden reflectivity drop on the seismic sections presented in the depth domain. Some reflections might ~~find their continuation in~~continue into the upper mantle, ~~like~~such as events visible ~~at~~on line 5600 and 1200, between CDP 1-2000 and 13500-14500, respectively. Some of the weaker sub-Moho reflectivity might be related to the migration artefacts or other processing footprints, however, the stronger ones (e.g. the one at line 5600) ~~seems~~seem to be real.

5 Discussion and preliminary interpretation

The reprocessed PolandSPAN™ profiles from NE Poland ~~are showing~~show a much more complex architecture of the EEC crust ~~as~~ compared with the WARR data (Grad et al., 2010), which is ~~not surprising given the methodology employed in the case of near vertical incidence reflection profiling and WARR acquisition and modelling.~~a result of the different methodologies employed. However, as discussed below, it is not only an issue of more complex reflectivity observed in the reflection profiles but also a redefinition of the middle/lower crust and Moho depths.

The thickness of the Phanerozoic platform cover varies from ~7-8 km in the SW to less than 2 km in the NE (Fig. 7~~ and 8~~-9). With few exceptions (e.g. SW part of line 5400, Fig. 8), reflection Moho is relatively well defined as ~~a band~~the base of ~~reflectors~~bands of intermittent reflections dividing reflective crust from the generally more transparent upper mantle. In the following comparisons, we use the compilation of WARR data by Majdański (2012), including the top lower crust and Moho horizons. The depth to WARR Moho varies smoothly along the interpreted PolandSPAN™ profiles between 38 and 43 km with a typical value around 40 km, being close to the global average of the "normal" continental crust (Christensen and Mooney, 1995). The agreement between such defined WARR Moho and the assumed crust-mantle boundary interpreted in the reflection data is good, with some notable exceptions. Reflection Moho along line 1200 is ~2-3 km shallower than the WARR Moho (Fig. 7). Reflection Moho in the NE part of line 5600 is up to 4 km shallower. Reflection Moho along line 5500 is ~2 km shallower. In the case of line 5400, ~~there is~~ a Moho uplift (~2-3 km) is observed ~~(see~~. See discussion on the AMCG complex below~~).~~. However, considering the fact that the velocities in the ~~sediments~~sedimentary cover are poorly resolved in WARR models and we used ~~here~~ reflection-derived velocities ~~for sediments~~at shallower depths, those changes can be attributed to the differences between those two methods. The depth to lower crust was inferred using WARR data and the change in the reflectivity patterns observed between the middle/lower crustal depths. The lower crust has generally a much-reduced thickness as compared with the WARR model. We can note some distinct lower crustal reflectivity patterns, with a common observation that the lower crust is reflective close to its top.

Black lines in Figs. 7-9 delineate representative reflection fabrics and shear zones, which we infer from the data. The main type of reflections corresponds to the gently dipping to subhorizontal structural layering, presumably representing ~~Svekofenian~~Svekofennian orogenic fabric (labelled S in Figs. 7~~, 8~~-9). A number of low-angle ~~detachments~~discontinuities (15-20~~°~~)°), inferred from the seismic reflections, branch off from the subhorizontal fabric, being followed by sub-parallel layering. These ~~detachments~~features, probably matching ductile thrust shear zones, are dipping towards NE and SE in the NE-SW and NW-SE oriented sections, respectively (labelled T in Figs. 7~~, 8~~-9). Collectively, their geometry is consistent with the previously postulated SW to W polarity of the ~~Svekofenian~~Svekofennian orogen (e.g., Park, 1985; Gorbatschev and Bogdanova, 1993; Korja and Heikkinen, 1995, 2005; Nironen, 1997). The SW-ward polarity of the orogen is also in accord with the NE dipping upper mantle reflectors that may correspond to the preserved relics of a Paleoproterozoic subduction zone. In several places, at a lower/middle crust level, the subhorizontal reflectors or NE-dipping shear zones are truncated by a package of reflectors with an opposite, i.e., NW- or SW-directed dip, e.g. line 1200 between CDP 1000-~~4000~~5000 (Fig. 7) and line 5400 between CDP ~~9000~~8000-12000 (Fig. 8). These SW-dipping events comprise straight reflections flanked by

reflections bent into parallelism with the SW-inclined packages. Consequently, subhorizontal or NE-dipping sets of reflectors often acquire a sigmoidal shape with terminations aligned into the SW-dipping events. The latter presumably correspond to extensional or transtensional shear zones of uniform geometry and kinematics throughout the studied sections. Both sets of structures identified in the seismic images jointly delineate a kilometer-scale S-C' fabric (Fig. 10) related to the SW-directed (in the present-day coordinates) mid- and lower crustal flow. The subhorizontal to NE dipping, often sigmoidal reflectors represent first-order orogen-scale shear planes (S), whereas the SW-dipping events correspond to extensional shear zones (C') produced during orogen-scale non-coaxial flow~~.~~ (Fig. 10). A similar fabric was described by Torvela et al. (2013) for the FIRE profiles onshore Finland. These authors link the structural pattern observed to the overall convergent tectonic setting of the accretionary Svecofennian orogeny (1.96–1.76 Ga; Korja and Heikkinen, 1995, 2005; Torvela et al., 2013). Following classical studies by Beaumont et al. (2001) and Vanderhaege and Teyssier (2001), Torvela et al. (2013) postulate syn-convergent flow of hot lower and middle crust comparable to that presently connected with the Tibetan Plateau (e.g., Beaumont et al., 2001, 2006; Lee and Whitehouse, 2007). According to these models, partial melting of thermally mature thickened orogenic crust and associated widspread migmatisation results in the generation of low-viscosity crustal layer that may undergo extension in an overall convergent setting (e.g., Beaumont et al., 2001; Vanderhaege and Teyssier, 2001). Drill core data from the Paleoproterozoic basement of NE Poland actually confirm widspread migmatisation and syn-orogenic magmatism at the time of the ~~Svekofenian~~Svekofennian orogeny (Krzemińska et al., 2017).

We favour syn-convergent crustal flow explanation over late- to post-orogenic extensional collapse (Korja and Heikkinen, 1995, 2005) ~~also because of~~due to the structural record from the AMCG igneous suite (Cymerman, 2004, 2014). Structural analysis of drill cores suggests localized compressive deformation of the Mesoproterozoic (1.54-1.45 Ga) AMCG intrusions (Cymerman, 2004, 2014) implying cessation of orogenic-scale extension by the time of their emplacement. Formation of the S-C' fabric, revealed by the seismic data, must have been already accomplished before the AMCG magmatism. Furthermore, seismic-scale deformational features are not imaged within the plutons (Figs. 7~~, 8~~-9). However, some possible contacts of the AMCG bodies coincide with zones of increased crustal reflectivity suggesting that reactivation of inherited shear zones may have provided conduits for emplacement of magma. Consequently, we propose that delamination of ~~overthickened~~over-thickened Svecofenian lithosphere may have accounted for underplating of gabbroic magma that fractionated into the AMCG plutons in NE Poland, following classical models of ~~the~~ AMCG magmatism ~~(see~~. See McLelland et al~~.,~~. (2010) for review~~).~~. The gabbroic parental magma yielded anorthositic derivatives subsequently ascending into the middle to upper crust together with granitoids derived by crustal anatexis (e.g., McLelland et al., 2010). ~~—~~Increased mantle reflectivity ~~below~~in the vicinity of the AMCG bodies~~, observed both for line 1200 and 5400 (marked by the ellipse in Figs. 7-8), could be related to~~ may signify fragments of delaminated lower crustal material. Sub-Moho reflectivity was also observed along the POLONAISE'97 P4 profile between P3 and P5 profiles (Grad et al., 2002). The exact shape of ~~the~~a lower/middle crustal gabbroic body and its position with respect to the inferred subcrop of the MC AMCG rocks is likely controlled by the interplay between the magmatism and the structure developed during the Palaeoproterozoic collisional and post-collisional deformations – a mechanism suggested for the Korosten Pluton by Bogdanova et al. (2004). Bright lower crustal reflectors and their complex shape (with some truncations) observed in the vicinity of the AMCG suite along lines 1200 and 5400 seems to support such an idea. We have to point out, that the interpreted shapes of the AMCG bodies in Figures 7-9 are only tentative and rely on coincidence of three evidences: (1) presence of mostly transparent crust in seismic sections, (2) occurrence of the AMCG suite outcrops at the top of the basement (after Krzemińska et al., 2017), and (3) concurrence of magnetic highs (Figs 3, 7-9) due to elevated magnetic susceptibility of the AMCG rocks.

~~There is an~~An interesting reflector (marked ~~S~~SI in Fig. 8) is observed along line 5400 for more than 60 km between CDPs 5000-10000 at a depth of ~7-9 km. It was also visible in the original ION Geophysical time/depth imaging, as well as in the industry seismic data from this area (P. Krzywiec, pers. comm.). It is offset with respect to the magnetic high crossed by line

5400 (Fig. 3). The S reflector can be tentatively linked with the AMCG intrusion, representing a sill (or top of the layered intrusion) fed by the mafic dykes as in the Shumlyanskyy's et al. (2017) model for the Korosten Pluton in Ukraine. An alternative explanation invokes a much younger magmatic event. Since the lower Carboniferous syenite intrusion of the Olsztyn Massif (Fig. 2) is less than 100 km to the SE of line 5400, the ~~S~~SI-reflector (and associated deeper subhorizontal reflectors) can be alternatively interpreted as intrusions of this age. Such an explanation of the ~~S~~SI-reflector origin is also supported by the fact that the lower Carboniferous sills were drilled offshore Lithuania (Motuza et al~~.~~., 2015).

The BABEL seismic profiles in the Baltic Sea imaged several dipping sub-Moho reflectors projecting into the Fennoscandian mantle (Abramovitz et al., 1997; BABEL Working Group, 1993; Balling, 2000; Korja and Heikkinen, 2005). The pronounced dipping mantle reflector observed NE of the Bornholm area along the BABEL A line (from 40 to 65 km depth) was interpreted by Balling (2000) as a relic of paleosubduction occurring at ~1.8-1.7 Ga. The same reflections projecting into the mantle were also imaged by the DEKORP-PQ profiles parallel to the BABEL A profile close to Bornholm and they were also attributed to the Proterozoic terrane accretion (Krawczyk et al., 2002; Meissner and Krawczyk, 1999). Projecting the BABEL A and PQ mantle reflectors to line 5600, suggests that we may observe the same feature at the SW end of this profile. Krawczyk et al. (2002) concluded that the Baltica crust was not mechanically involved in the Caledonian collision. This view can be supported by the recent study by Mazur et al. (2016b), who suggested that the CDF is a thin-skinned feature. Therefore, we do not link the observed reflectivity patterns (including mantle reflectors) with ~~the~~ Caledonian ~~deformations~~deformation, but consider them to represent a Proterozoic accretion signature.

6 Conclusions

Reprocessing of ~950 km of the regional seismic profiles from the PolandSPAN™ project provided for the first time a detailed picture of the EEC (Fennoscandian) crust in NE Poland. It revealed reflectivity patterns that we primarily associate with ~~the~~ Paleoproterozoic ~~crust~~crustal formation during the Svekofennian (Svekobaltic) ~~orogeny~~Orogeny, and which are similar to ~~what is~~those observed along the BABEL and FIRE profiles in the Baltic Sea and onshore Finland, respectively (Korja and Heikkinen, 2005; Torvela et al., 2013). We suggest that a seismic-scale S-C' fabric of the Paleoproterozoic crust was shaped by mid- to lower-crustal flow in a convergent setting during the Svecofenian orogeny. We propose that delamination of the ~~overthickened~~thickened Svecofennian lithosphere and resulting asthenospheric ascent, partial melting of lithospheric mantle and ponding of gabbroic melt at the crust–mantle interface (McLelland et al., 2010) can be reconciled with the crustal fabric observed and explain the emplacement of the Mesoproterozoic AMCG suites in NE Poland. We also found sub-Moho dipping mantle reflectivity, which we tentatively explain as a signature of paleosubduction occurring prior to the Svekofennian orogeny. Later tectonic phases (e.g. Ediacaran rifting, Caledonian orogeny) did not leave a clear signature in the deeper crust, however, some of the subhorizontal reflectors below the basement ~~can~~may be linked with a lower Carboniferous magmatism.

Author contribution

Conceptualization, MMal; Methodology, MM & MMal.; Software, MM; Validation, MM & MMal.; Formal Analysis, MM, MMal & SM; Investigation, MM & MMal.; Resources, MMal; Data Curation, MM & MMal; Writing – Original Draft Preparation, MM, MMal & SM.; Writing – Review & Editing, MM, MMal & SM; Visualization, MM, MMal & SM.; Supervision, MMal; Project Administration, MMal.; Funding Acquisition, MMal.

Competing interests

The authors declare that they have no conflict of interest

Acknowledgments

This study was funded by the Polish National Science Centre grant no UMO-2015/19/B/ST10/01612. We are grateful to A. Calvert for sharing his coherency filtration and segment migration codes with us. We are indebted to ION Geophysical for permission to use and show PolandSPAN™ data. Processing was done using GlobeClaritas™ software under the license from GNS Science, New Zealand. Comments from the two anonymous reviewers are greatly appreciated.

References

Abramovitz, T., Berthelsen, A. and Thybo, H.: Proterozoic sutures and terranes in the southeastern Baltic Shield interpreted from BABEL deep seismic data, Tectonophysics, 270(3–4), 259–277, doi:10.1016/S0040-1951(96)00213-2, 1997.

BABEL Working Group: Deep Seismic Reflection/Refraction Interpretation of Crustal Structure Along Babel Profiles A and B In the Southern Baltic Sea: Babel Working Group*, Geophys. J. Int., 112(3), 325–343, doi:10.1111/j.1365-246X.1993.tb01173.x, 1993.

Balling, N.: Deep seismic reflection evidence for ancient subduction and collision zones within the continental lithosphere of Northwestern Europe, Tectonophysics, 329(1–4), 269–300, doi:10.1016/S0040-1951(00)00199-2, 2000.

Barnes, A. E.: Moho reflectivity and seismic signal penetration, Tectonophysics, 232(1–4), 299–307, doi:10.1016/0040-1951(94)90091-4, 1994.

Beaumont, C., Jamieson, R.A., Nguyen, M.H. and Lee, B.: Himalayan tectonics explained by extrusion of a low-viscosity crustal channel coupled to focused surface denudation, Nature, 414, 738–742, 2001.

Beaumont, C., Nguyen, M.H., Jamieson, R.A. and Ellis, S.: Crustal flow modes in large hot orogens. Geological Society, London, Special Publications, 268(1), 91–145, 2006.

Bogdanova, S., Gorbatschev, R., Skridlaite, G., Soesoo, A., Taran, L. and Kurlovich, D.: Trans-Baltic Palaeoproterozoic correlations towards the reconstruction of supercontinent Columbia/Nuna, Precambrian Res., 259, 5–33, doi:10.1016/J.PRECAMRES.2014.11.023, 2015.

Bogdanova, S. V., Pashkevich, I. K., Buryanov, V. B., Makarenko, I. B., Orlyuk, M. I., Skobelev, V. M., Starostenko, V. I. and Legostaeva, O. V.: The 1.80–1.74-Ga gabbro–anorthosite–rapakivi Korosten Pluton in the Ukrainian Shield: a 3-D geophysical reconstruction of deep structure, Tectonophysics, 381(1–4), 5–27, doi:10.1016/J.TECTO.2003.10.023, 2004.

Bogdanova, S. V., Bingen, B., Gorbatschev, R., Kheraskova, T. N., Kozlov, V. I., Puchkov, V. N. and Volozh, Y. A.: The East European Craton (Baltica) before and during the assembly of Rodinia, Precambrian Res., 160(1–2), 23–45, doi:10.1016/j.precamres.2007.04.024, 2008.

Calvert, A. J.: A method for avoiding artifacts in the migration of deep seismic reflection data, Tectonophysics, 388(1–4), 201–212, doi:10.1016/J.TECTO.2004.07.026, 2004.

Christensen, N. I. and Mooney, W. D.: Seismic velocity structure and composition of the continental crust: a global view, J. Geophys. Res., 100(B6), 9761–9788, doi:10.1029/95JB00259, 1995.

Cymerman, Z.: Precambrian of the Polish part of the East European Platform: tectonics and crustal development [in Polish, English summary]. Prace Państwowego Instytutu Geologicznego, CLXXX, 1–129, 2004.

Cymerman, Z.: Structural and kinematic analysis and the Mesoproterozoic tectonic evolution of the Suwałki basic massif and its surroundings, NE Poland [in Polish, English summary]. Prace Państwowego Instytutu Geologicznego, 201, 1–167, 2014.

Czuba, W., Grad, M., Luosto, U., Motuza, G., Nasedkin, V., Guterch, A., Środa, P., Keller, G. R., Thybo, H., Türa, T., Yliniemi, J., Lund, C. E., Jacyna, J., Korabliova, L. and Nasedkin, V.: Upper crustal seismic structure of the Mazury complex and Mazowsze massif within East Europe Craton in NE Poland, Tectonophysics, 360(1–4), 115–128, doi:10.1016/S0040-1951(02)00352-9, 2002.

Dadlez, R., Kowalczewski, Z. and Znosko, J.: Some key problems of the pre-Permian tectonics of Poland, Geol. Quart., 38(2), 169–190, 1994.

Dörr, W., Belka, Z., Marheine, D., Schastok, J., Valverde-Vaquero, P. and Wiszniewska, J.: U–Pb and Ar–Ar geochronology of anorogenic granite magmatism of the Mazury complex, NE Poland, Precambrian Res., 119(1–4), 101–120, doi:10.1016/S0301-9268(02)00119-5, 2002.

Dziewinska, L. and Tarkowski, R.: Geophysical study of deep basement structure of NW Poland using effective reflection coefficients, Comptes Rendus Geosci., 348(8), 587–597, doi:10.1016/J.CRTE.2016.06.003, 2016.

Fossen, H.: Structural Geology, Cambridge University Press, 2016.

Gorbatschev, R. and Bogdanova, S.: Frontiers in the Baltic Shield, Precambrian Res., 64(1–4), 3–21, doi:10.1016/0301-9268(93)90066-B, 1993.

Grad, M., Keller, Thybo, H. and Guterch, A.: Lower lithospheric structure beneath the Trans-European Suture Zone from POLONAISE'97 seismic profiles, Tectonophysics, 360(1–4), 153–168, doi:10.1016/S0040-1951(02)00350-5, 2002.

Grad, M., Jensen, S. L., Keller, G. R., Guterch, A., Thybo, H., Janik, T., Tiira, T., Yliniemi, J., Luosto, U., Motuza, G., Nasedkin, V., Czuba, W., Gaczyński, E., Środa, P., Miller, K. C., Wilde- Piórko, M., Komminaho, K., Jacyna, J. and Korabliova, L.: Crustal structure of the Trans-European suture zone region along POLONAISE'97 seismic profile P4, J. Geophys. Res., 108(B11), 2541, doi:10.1029/2003JB002426, 2003.

Grad, M., Janik, T., Guterch, A., Środa, P. and Czuba, W.: Lithospheric structure of the western part of the East European Craton investigated by deep seismic profiles, Geol. Q., 50(1), 9–22, 2010.

Grad, M., Polkowski, M. and Ostaficzuk, S. R.: High-resolution 3D seismic model of the crustal and uppermost mantle structure in Poland, Tectonophysics, 666, 188–210, doi:10.1016/J.TECTO.2015.10.022, 2016.

Guterch, A., Grad, M., Janik, T., Materzok, R., Luosto, U., Yliniemi, J., Lück, E., Schulze, A. and Förste, K.: Crustal structure of the transition zone between Precambrian and Variscan Europe from new seismic data along LT-7 profile (NW Poland and eastern Germany), C. R. Acad. Sci. Paris, 319, 1489–1496, 1994.

Janik, T., Yliniemi, J., Grad, M., Thybo, H., Tiira, T., Gaczyński, E., Guterch, A., Keller, G. R. and Komminaho, K.: Crustal structure across the TESZ along Polonaise'97 seismic profile P2 NW Poland, Tectonophysics, 360(1–4), 129–152, doi:10.1016/S0040-1951(02)00353-0, 2002.

Johansson, Å.: Baltica, Amazonia and the SAMBA connection—1000 million years of neighbourhood during the Proterozoic?, Precambrian Res., 175(1–4), 221–234, doi:10.1016/J.PRECAMRES.2009.09.011, 2009.

Korja, A. and Heikkinen, P.: The accretionary Svecofennian orogen—insight from the BABEL profiles, Precambrian Res., 136(3–4), 241–268, doi:10.1016/J.PRECAMRES.2004.10.007, 2005.

Korja, A. and Heikkinen, P. J.: Proterozoic extensional tectonics of the central Fennoscandian Shield: Results from the Baltic and Bothnian Echoes from the Lithosphere experiment, Tectonics, 14(2), 504–517, doi:10.1029/94TC02905, 1995.

Krawczyk, C. ., Eilts, F., Lassen, A. and Thybo, H.: Seismic evidence of Caledonian deformed crust and uppermost mantle structures in the northern part of the Trans-European Suture Zone, SW Baltic Sea, Tectonophysics, 360(1–4), 215–244, doi:10.1016/S0040-1951(02)00355-4, 2002.

Krzemińska, E., Krzemiński, L., Petecki, Z., Wiszniewska, J., Salwa, S., Żaba, J., Gaidzik, K., Williams, I.S., Rosowiecka, O, Taran, L., Johansson, Å., Pécskay, Z., Demaiffe, D., Grabowski, J. and Zieliński, G.: Geological Map of Crystalline Basement in the Polish part of the East European Platform 1:1 000 000. Państwowy Instytut Geologiczny. Warszawa, 2017.

Krzywiec, P., Lis, P., Buffenmyer, V., Malinowski, M. and Lewandowski, M.: Regional Geologic Characterization of the Polish Lower Paleozoic Unconventional Play Using an Integrated Seismic and Well Data Approach, in Unconventional Resources Technology Conference, Denver, Colorado, 12-14 August 2013, pp. 183–187, Society of Exploration Geophysicists, American Association of Petroleum Geologists, Society of Petroleum Engineers., 2013.

Krzywiec, P., Mazur, S., Gągała, Ł., Kufrasa, M., Lewandowski, M. and Malinowski, Michał Buffenmyer, V.: Late

Carboniferous thin-skinned compressional deformation above the SW edge of the East European craton as revealed by seismic reflection and potential field data—Correlations with the Variscides and the Appalachians, in GSA Memoirs: Linkages and Feedbacks in Orogenic Systems, vol. 213, pp. 353–372, Geological Society of America., 2017a.

Krzywiec, P., Gągała, Mazur, S., Słonka, Kufrasa, M., Malinowski, M., Pietsch, K. and Golonka, J.: Variscan deformation along the Teisseyre-Tornquist Zone in SE Poland: Thick-skinned structural inheritance or thin-skinned thrusting?, Tectonophysics, 718, 83–91, doi:10.1016/j.tecto.2017.06.008, 2017b.

Kukkonen, I. T. and Lahtinen, R.: Finnish reflection experiment FIRE 2001-2005, Geological Survey of Finland., 2006.

Lahtinen, R., Korja, A., Nironen, M. and Heikkinen, P.: Palaeoproterozoic accretionary processes in Fennoscandia, Geol. Soc. London, Spec. Publ., 318(1), 237–256, doi:10.1144/SP318.8, 2009.

Lee, J. and Whitehouse, M.J.: Onset of mid-crustal extensional flow in southern Tibet: Evidence from U/Pb zircon ages, Geology, 35(1), 45–48, 2007.

Majdański, M.: The structure of the crust in TESZ area by kriging interpolation, Acta Geophys., 60(1), 59–75, doi:10.2478/s11600-011-0058-5, 2012.

Malinowski, M.: Deep reflection seismic imaging in SE Poland using extended correlation method applied to PolandSPAN™ data, Tectonophysics, 689, 107–114, doi:10.1016/j.tecto.2016.01.007, 2016.

Malinowski, M. and Brettwood, P.: Using Extended Correlation Method in Regional Reflection Surveys - A Case Study from Poland, in 75th EAGE Conference & Exhibition incorporating SPE EUROPEC 2013 London, UK, 10-13 June 2013., 2013.

Malinowski, M., Guterch, A., Narkiewicz, M., Probulski, J., Maksym, A., Majdański, M., Środa, P., Czuba, W., Gaczyński, E., Grad, M., Janik, T., Jankowski, L. and Adamczyk, A.: Deep seismic reflection profile in Central Europe reveals complex pattern of Paleozoic and Alpine accretion at the East European Craton margin, Geophys. Res. Lett., 40(15), 3841–3846, doi:10.1002/grl.50746, 2013.

Malinowski, M., Guterch, A., Narkiewicz, M., Petecki, Z., Janik, T., Środa, P., Maksym, A., Probulski, J., Grad, M., Czuba, W., Gaczyński, E., Majdański, M. and Jankowski, L.: Geophysical constraints on the crustal structure of the East European Platform margin and its foreland based on the POLCRUST-01 deep reflection seismic profile, Tectonophysics, 653, 109–126, doi:10.1016/j.tecto.2015.03.029, 2015.

Mazur, S., Mikolajczak, M., Krzywiec, P., Malinowski, M., Buffenmyer, V. and Lewandowski, M.: Is the Teisseyre-Tornquist Zone an ancient plate boundary of Baltica?, Tectonics, 34(12), 2465–2477, doi:10.1002/2015TC003934, 2015.

Mazur, S., Mikolajczak, M., Krzywiec, P., Malinowski, M., Lewandowski, M. and Buffenmyer, V.: Pomeranian Caledonides, NW Poland – A collisional suture or thin-skinned fold-and-thrust belt?, Tectonophysics, 692, 29–43, doi:10.1016/j.tecto.2016.06.017, 2016a.

Mazur, S., Mikolajczak, M., Krzywiec, P., Malinowski, M., Buffenmyer, V. and Lewandowski, M.: Reply to Comment by M. Narkiewicz and Z. Petecki on "Is the Teisseyre-Tornquist Zone an ancient plate boundary of Baltica?," Tectonics, 35(6), 1600–1607, doi:10.1002/2016TC004162, 2016b.

McLelland, J.M., Selleck, B.W., Hamilton, M.A. and Bickford, M.E.: Late-to post-tectonic setting of some major Proterozoic anorthosite–mangerite–charnockite–granite (AMCG) suites, The Canadian Mineralogist, 48(4), 729–750, doi: 10.3749/canmin.48.4.000, 2010.

Meissner, R. and Krawczyk, C. H.: Caledonian and Proterozoic terrane accretion in the southwest Baltic Sea, Tectonophysics, 314(1–3), 255–267, doi:10.1016/S0040-1951(99)00247-4, 1999.

Mezyk, M. and Malinowski, M.: Deep Neural Network and Multi-pattern Based Algorithm for Picking First-arrival Traveltimes, in 80th EAGE Conference and Exhibition, Copenhagen., 2018.

Motuza, G., Šliaupa, S. and Timmerman, M. J.: Geochemistry and ^{40}Ar/^{39}Ar age of Early Carboniferous dolerite sills in the southern Baltic Sea, Est. J. Earth Sci., 64(3), 233, doi:10.3176/earth.2015.30, 2015.

Nironen, M.: The Svecofennian Orogen: a tectonic model, Precambrian Research, 86, 21–44, 1997.

Okaya, D. A. and Jarchow, C. M.: Extraction of deep crustal reflections from shallow Vibroseis data using extended correlation, GEOPHYSICS, 54(5), 555–562, doi:10.1190/1.1442682, 1989.

Park, A.F.: Accretion tectonism in the Proterozoic Svecokarelides of the Baltic Shield, Geology, 13, 725–729, 1985.

Poprawa, P., Šliaupa, S., Stephenson, R. and Lazauskiene, J.: Late Vendian-Early Palaeozoic tectonic evolution of the Baltic Basin: Regional tectonic implications from subsidence analysis, Tectonophysics, 314(1–3), 219–239, doi:10.1016/S0040-1951(99)00245-0, 1999.

Shumlyanskyy, L., Hawkesworth, C., Billström, K., Bogdanova, S., Mytrokhyn, O., Romer, R., Dhuime, B., Claesson, S., Ernst, R., Whitehouse, M. and Bilan, O.: The origin of the Palaeoproterozoic AMCG complexes in the Ukrainian shield: New U-Pb ages and Hf isotopes in zircon, Precambrian Res., 292, 216–239, doi:10.1016/J.PRECAMRES.2017.02.009, 2017.

Skridlaite, G., Wiszniewska, J. and Duchesne, J.-C.: Ferro-potassic A-type granites and related rocks in NE Poland and S Lithuania: west of the East European Craton, Precambrian Res., 124(2–4), 305–326, doi:10.1016/S0301-9268(03)00090-1, 2003.

Środa, P., Czuba, W., Guterch, A., Środa, P., Grad, M., Thybo, H., Keller, G. R., Miller, K. C., Tiira, T., Luosto, U., Yliniemi, J., Motuza, G. and Nasedkin, V.: P- and S-wave velocity model of the southwestern margin of the Precambrian East European Craton; POLONAISE'97, profile P3, in Tectonophysics, vol. 314, pp. 175–192., 1999.

Torvela, T., Moreau, J., Butler, R.W., Korja, A. and Heikkinen, P.: The mode of deformation in the orogenic mid- crust revealed by seismic attribute analysis, Geochemistry, Geophysics, Geosystems, vol. 14(4), pp.1069–1086, 2013.

Vanderhaege, O. and Teyssier, C.: Partial melting and flow of orogens, Tectonophysics, 342, 451–472, 2001.

Ziolkowski, A.: Review of vibroseis data acquisition and processing for better amplitudes: adjusting the sweep and deconvolving for the time-derivative of the true groundforce, Geophys. Prospect., 58(1), 41–54, doi:10.1111/j.1365-2478.2009.00841.x, 2010.

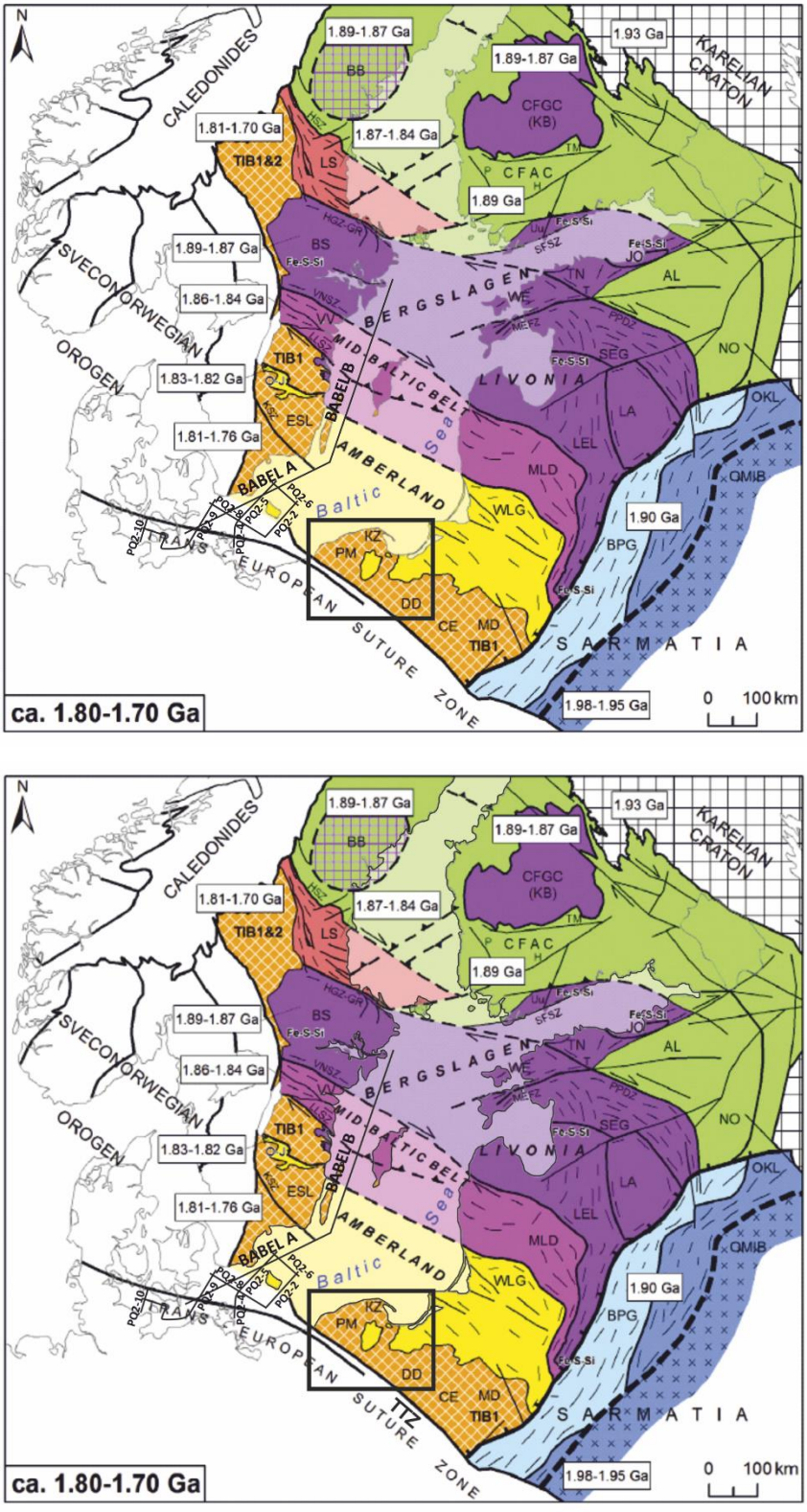

Figure 1: Major Paleoproterozoic tectonic domains of Fennoscandia across the Baltic Sea area. The black rectangle shows the study area. Location of the BABEL A/B (BABEL Working Group, 1993) and DEKORP-PQ (Meissner and Krawczyk, 1999) deep reflection profiles is also marked. The known extent of the domain affected by the Svecofennian orogeny (coloured terranes) is bounded by the Teisseyre-Tornquist Zone (TTZ) in the SW and the Belarus-Podlasie granulite belt (BPG) in the SE. Modified from Bogdanova et al. (2015).

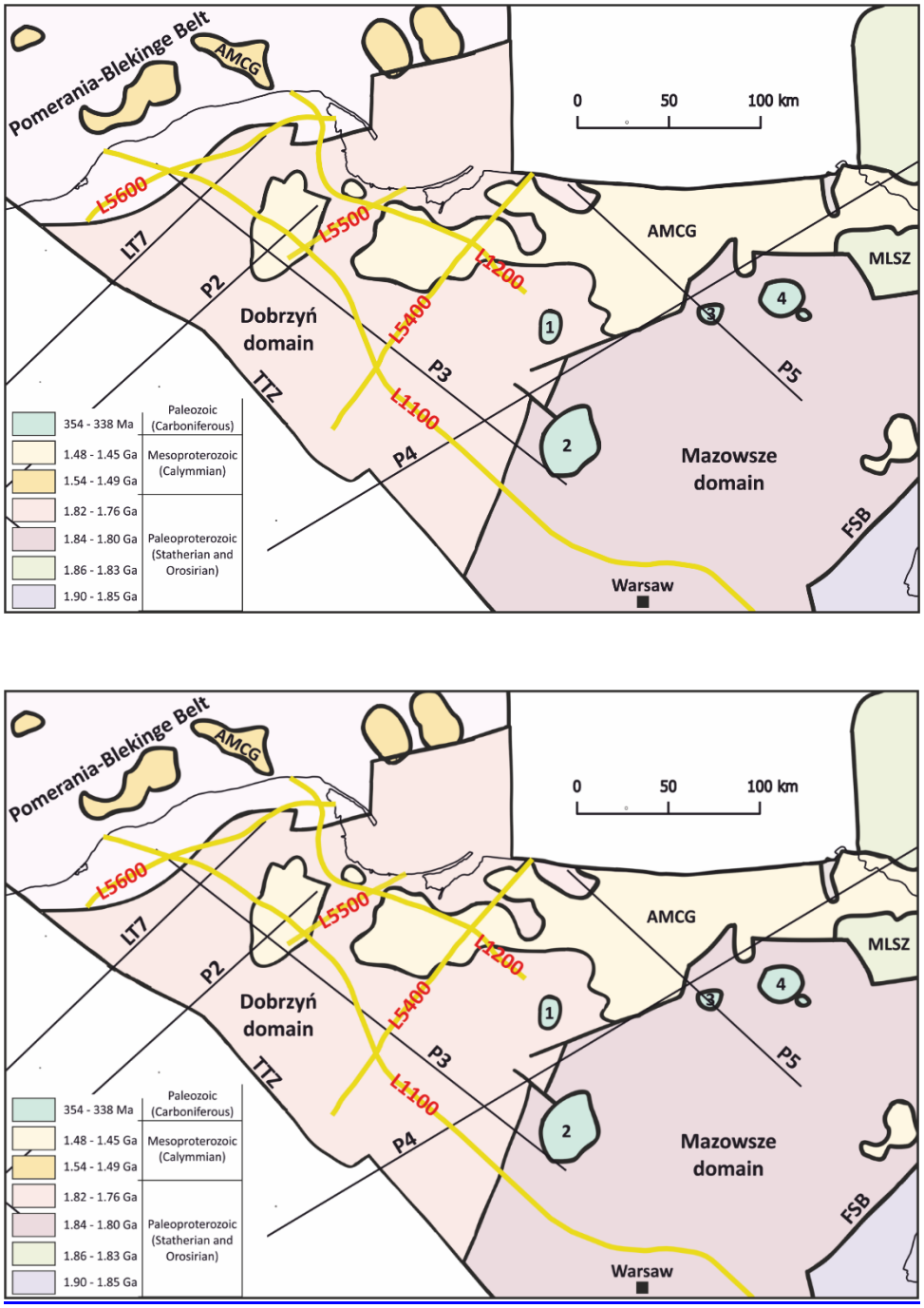

Figure 2: Location of the PolandSPAN™ seismic profiles (yellow lines) on the background of a simplified geological map of the East European Craton crystalline basement units (after Krzemińska et al., 2017). TTZ – Teisseyre-Tornquist Zone, FSB – Fennoscandia-Sarmatia boundary, AMCG - anorthosite-mangerite-charnockite granite complexes, MLSZ – Mid-Lithuanian Suture Zone, Paleozoic massifs: 1 – Olsztynek, 2 – Mława, 3- Pisz, 4 – Ełk. Locations of WARR profiles: LT7 (Guterch et al., 1994), POLANAISE'97 P2 (Janik et al., 2002), P3 (Środa et al., 1999), P4 (Grad et al., 2003) and P5 (Czuba et al., 2002) are marked as thin black lines.

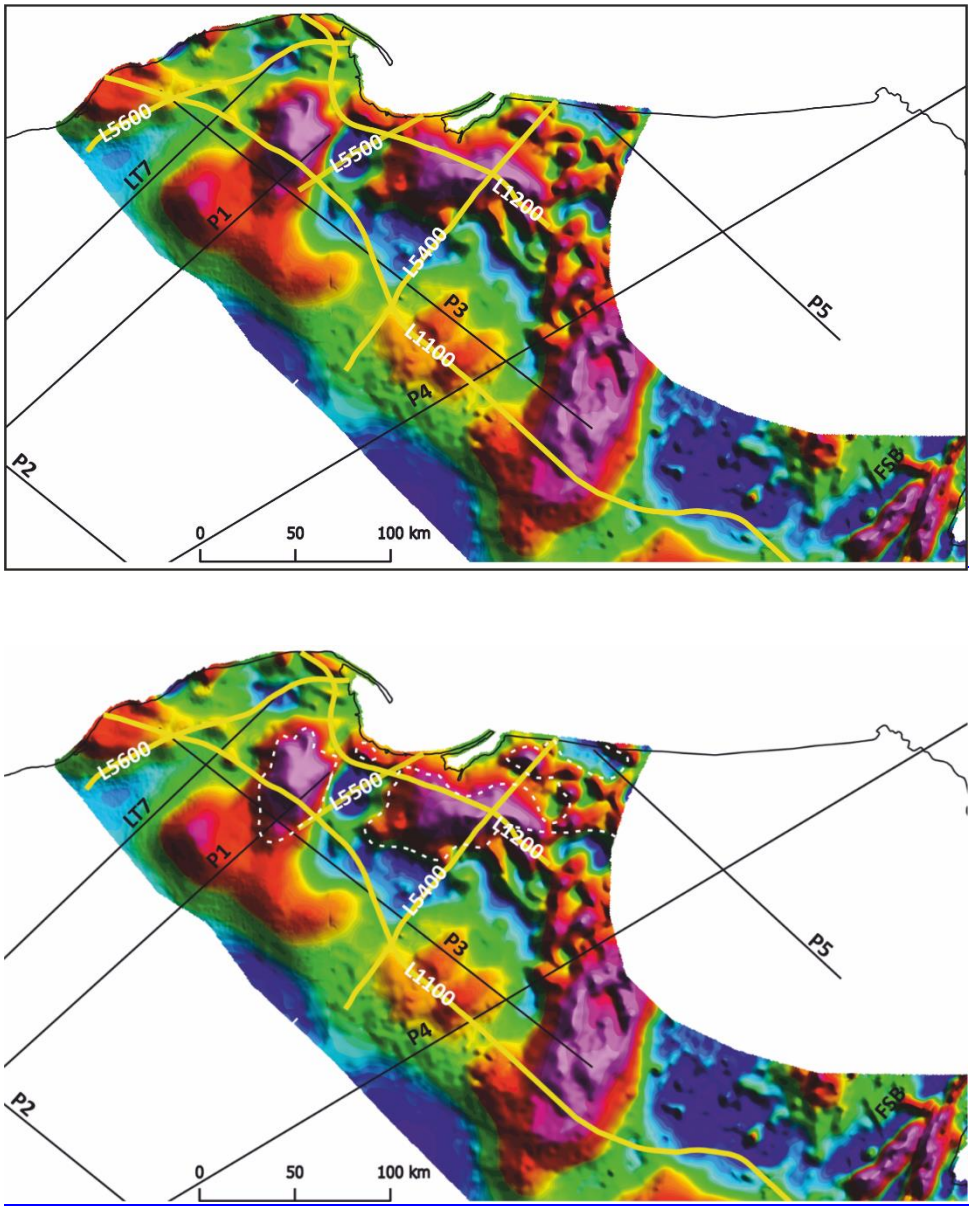

Figure 3: Location of the PolandSPAN™ seismic profiles on the background of a total magnetic field anomaly map of NE Poland (reduced to pole) (data compilation of S. Mazur). Location of the AMCG complexes from Fig. 2 is also indicated by a white dashed line.

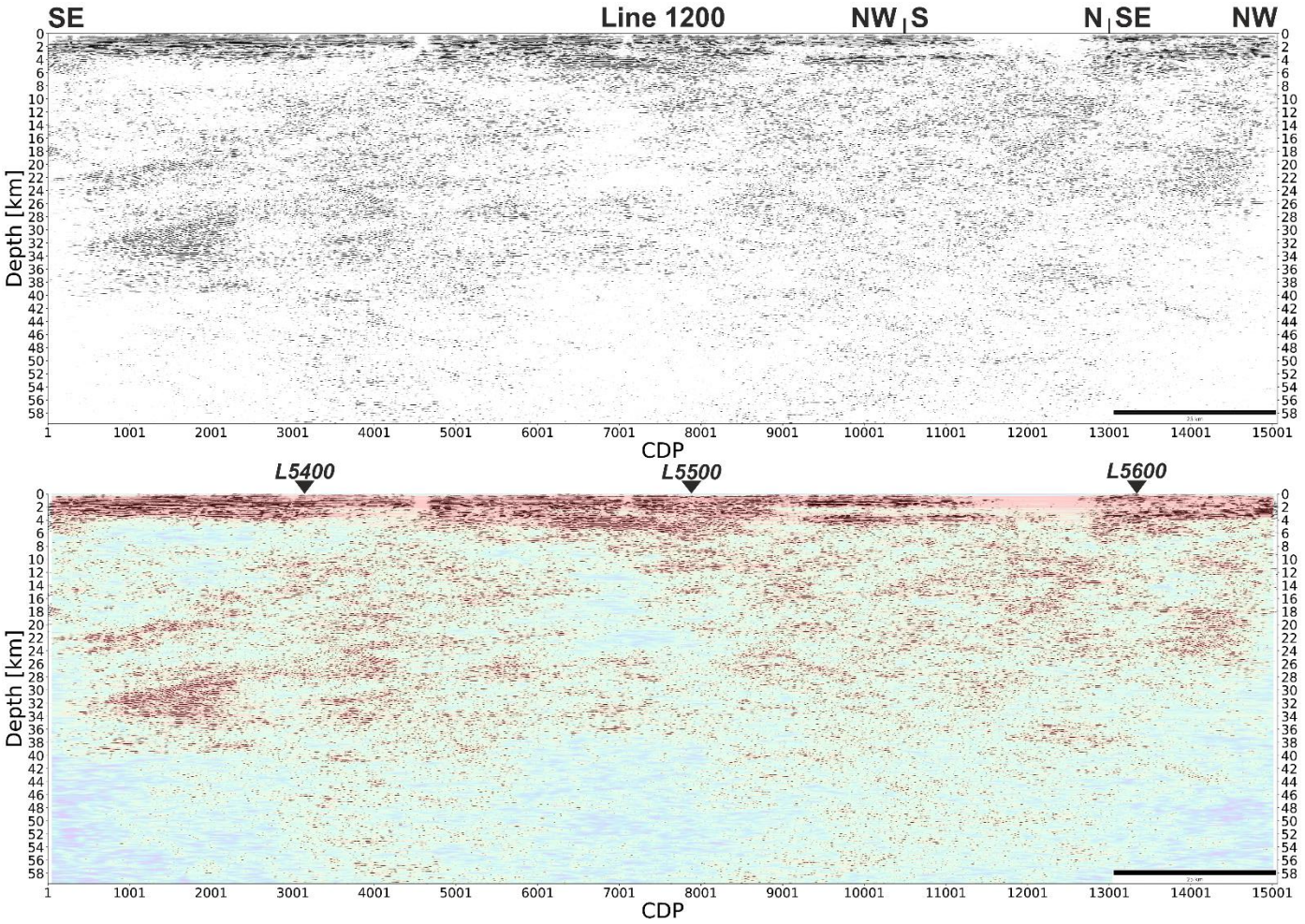
SE
Line 1200
NW
S
N
SE
NW
Depth [km]
CDP
L5400
L5500
L5600
Depth [km]
CDP

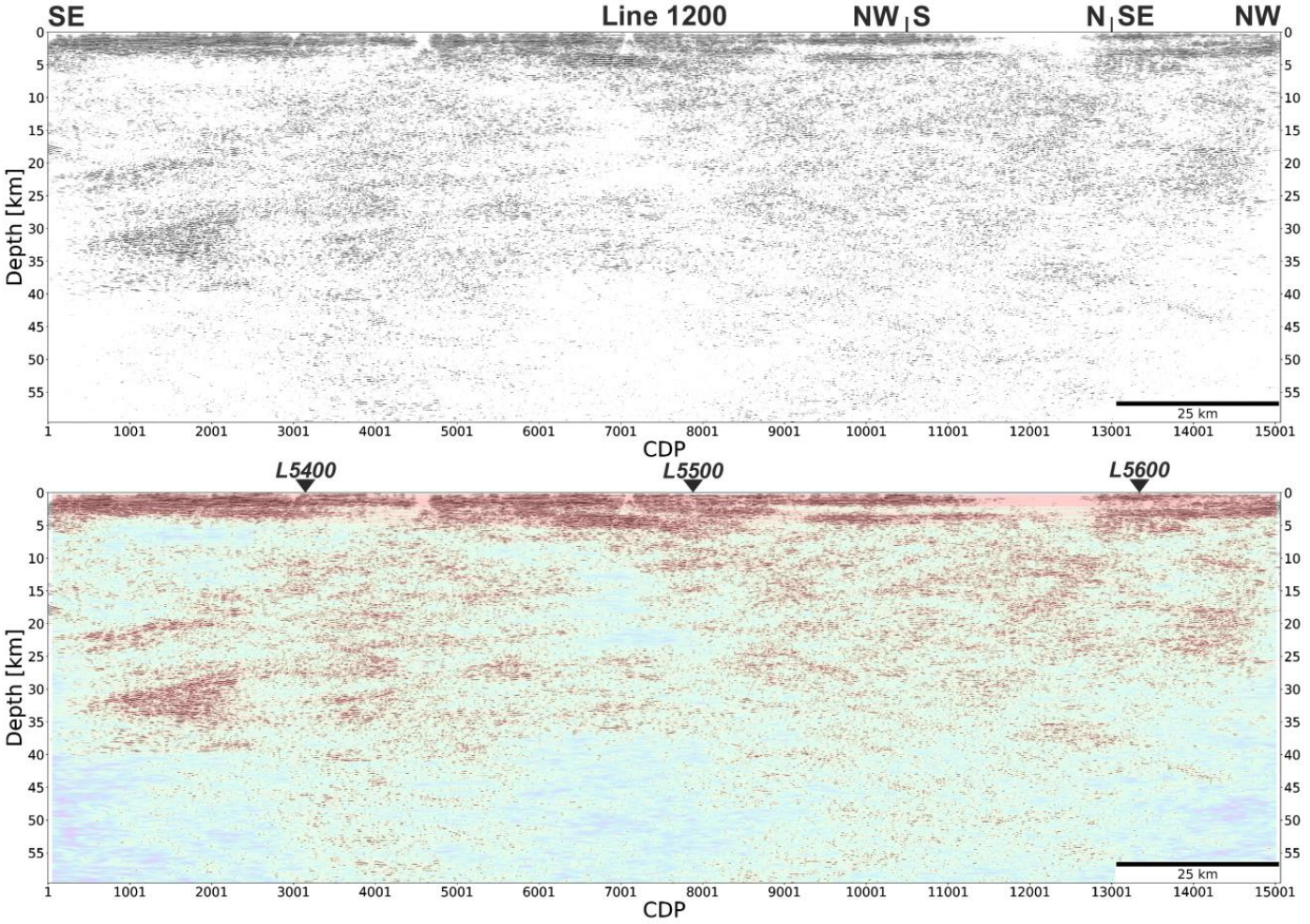

Figure 4: Final migrated depth-converted section along PolandSPAN™ profile 1200: a) plot of positive amplitudes, b) plot of positive amplitudes and amplitude envelope attribute in the background.

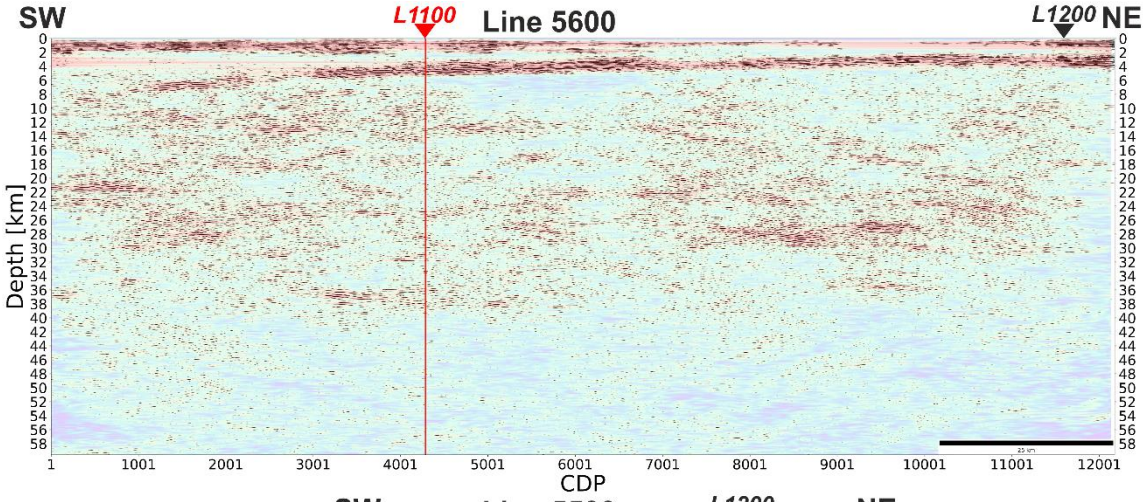
SW
L1100
Line 5600
L1200
NE
Depth [km]
CDP

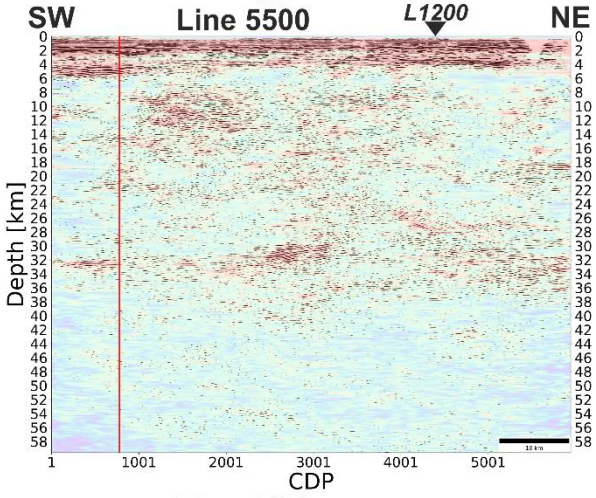
SW
Line 5500
L1200
NE
Depth [km]
CDP

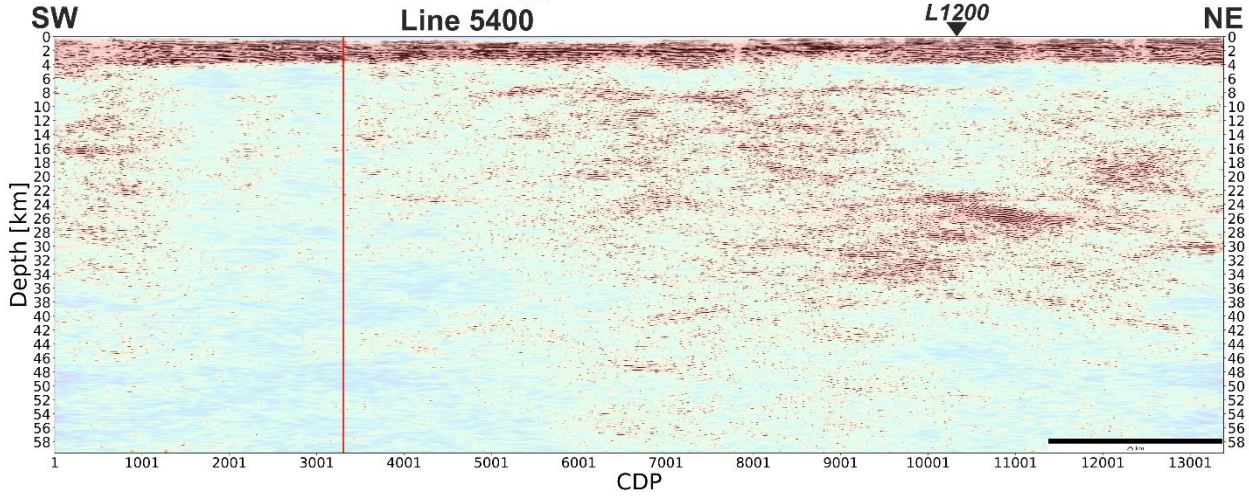
SW
Line 5400
L1200
NE
Depth [km]
CDP

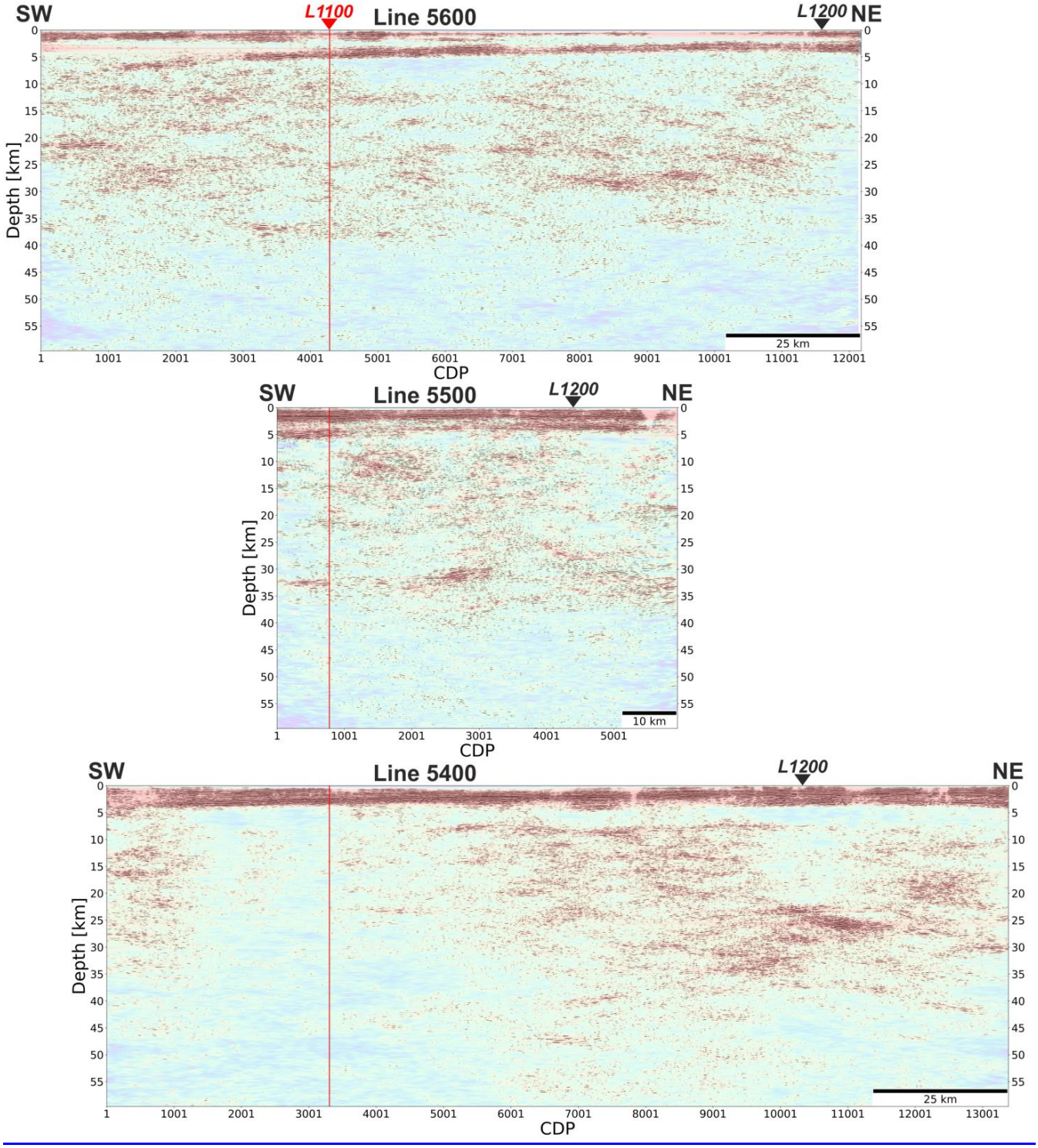

Figure 5: Final migrated depth-converted section along PolandSPAN™ profiles 5600, 5500 and 5400 (envelope and amplitude combined plot as in Fig. 4b). Profiles are centered at the intersection with line 1100 (vertical red line).

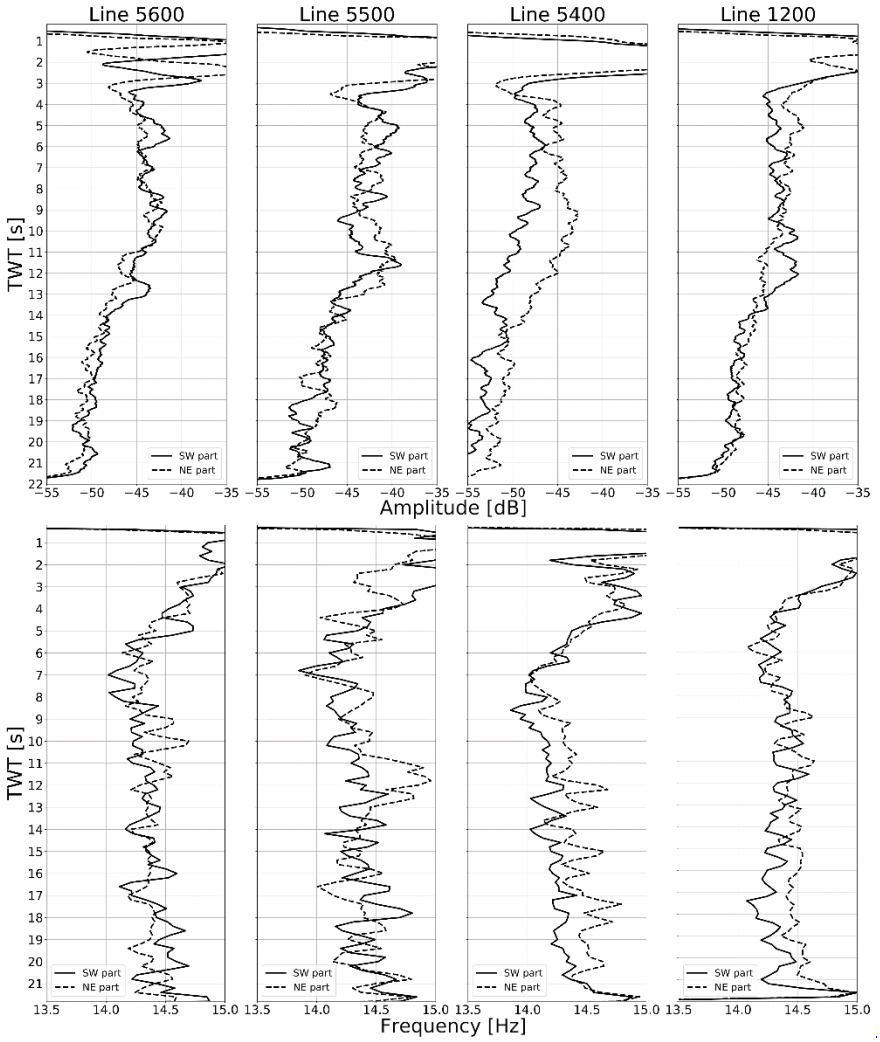
Line 5600
Line 5500
Line 5400
Line 1200
TWT [s]
SW part
NE part
Amplitude [dB]
Frequency [Hz]

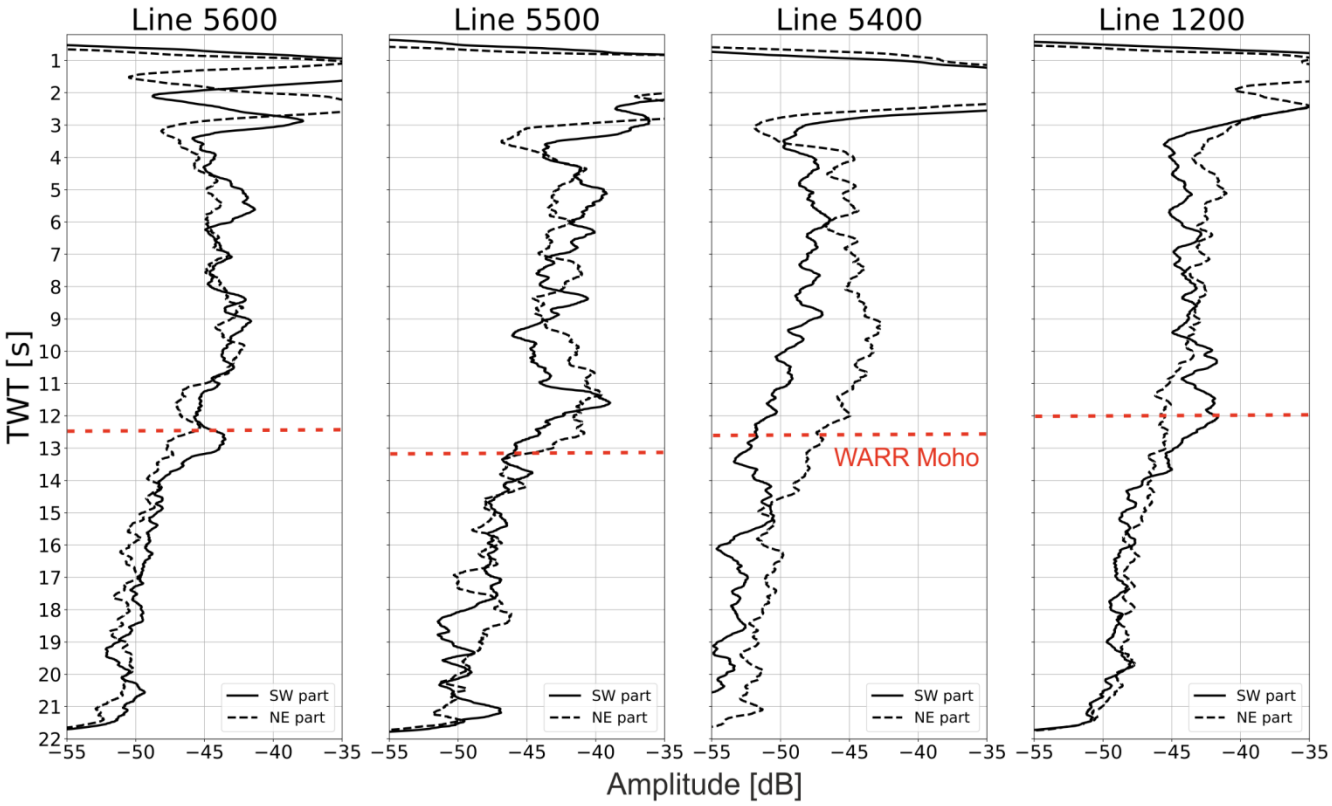

Figure 6: Amplitude ~~(top) and frequency (bottom)~~ decay curves extracted from ~~all~~ sections ~~from~~shown in Fig. 4 and 5.

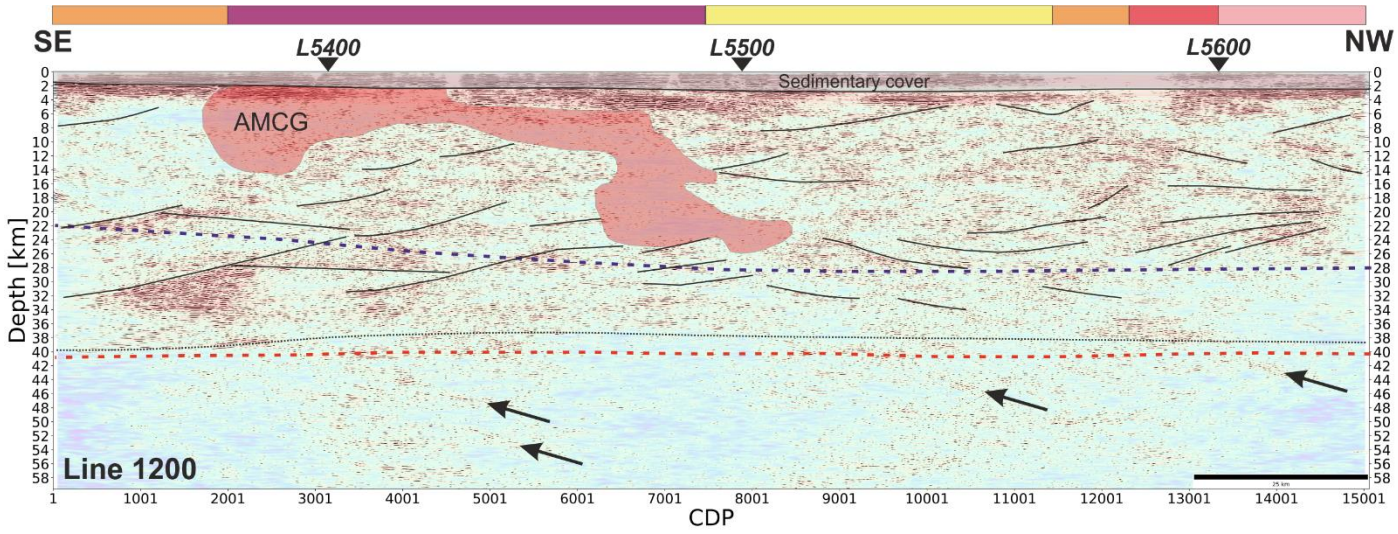

Red dashed line indicates average Moho depth inferred from WARR data.

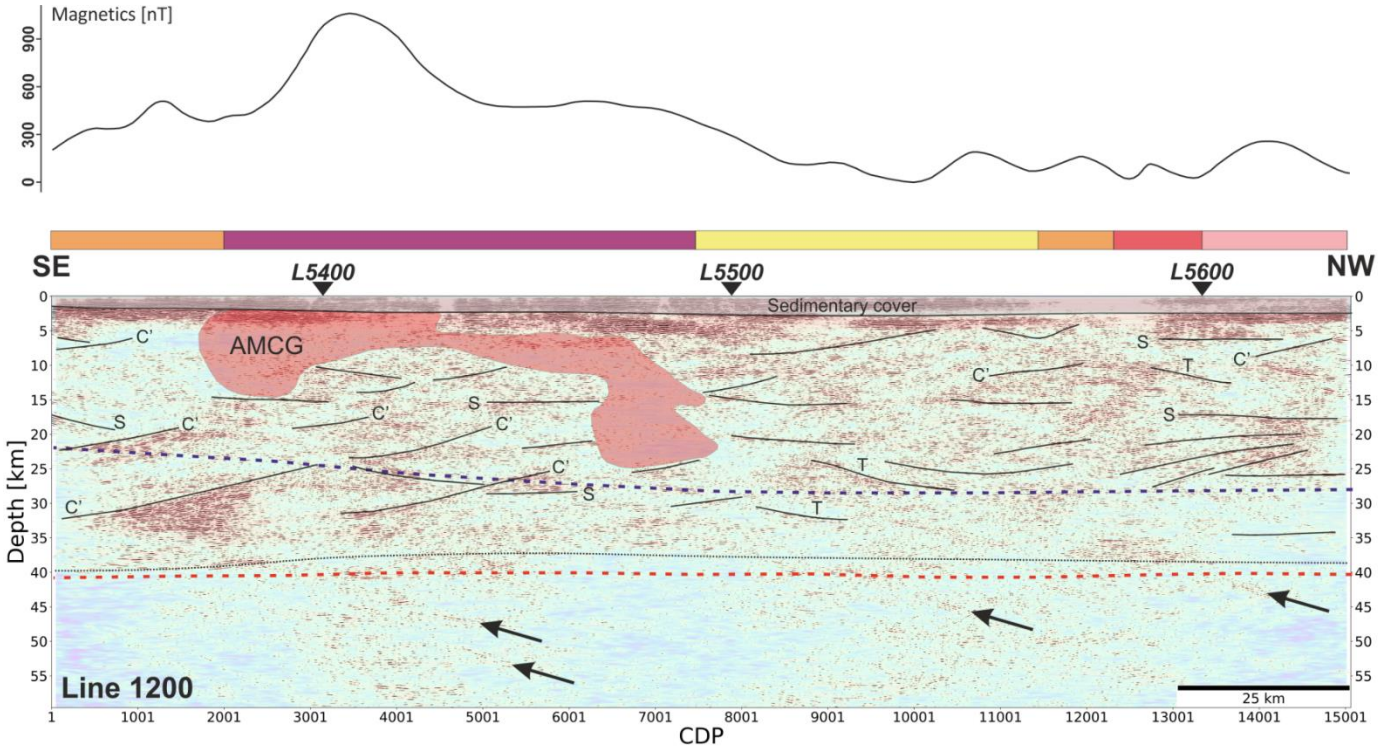

Figure 7: Final migrated depth-converted section along PolandSPAN™ profile 1200 with preliminary interpretation. Bars atop the section are colour-coded according to the crystalline basement lithologies following Krzemińska et al. (2017) (see Fig. ~~8~~9 for a legend). Magnetic profile at the top is extracted from the magnetic anomaly map (Fig. 3). Dashed ~~violet~~blue and red lines represent top of the lower crust and Moho boundary, respectively, taken from the WARR compilation of Majdański (2012). Black dotted line is the interpreted Moho boundary from reflection data. Arrows point to the upper mantle reflectors (RUM).

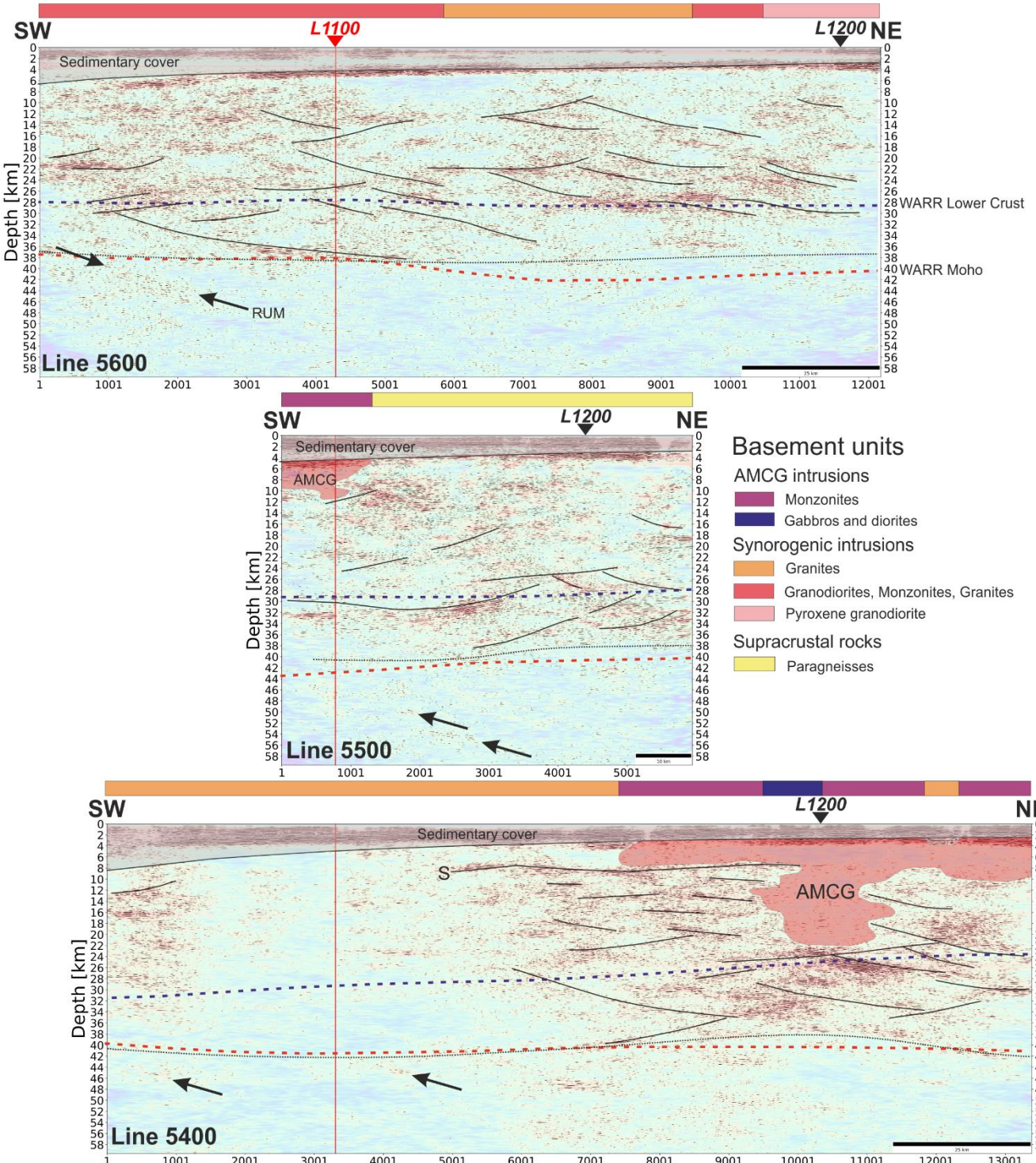
SW
L1100
L1200
NE
Sedimentary cover
Depth [km]
WARR Lower Crust
WARR Moho
RUM
Line 5600
1
1001
2001
3001
4001
5001
6001
7001
8001
9001
10001
11001
12001
SW
L1200
NE
Sedimentary cover
AMCG
Depth [km]
Line 5500
1
1001
2001
3001
4001
5001
Basement units
AMCG intrusions
Monzonites
Gabbros and diorites
Synorogenic intrusions
Granites
Granodiorites, Monzonites, Granites
Pyroxene granodiorite
Supracrustal rocks
Paragneisses
SW
L1200
NE
Sedimentary cover
S
AMCG
Depth [km]
Line 5400
1
1001
2001
3001
4001
5001
6001
7001
8001
9001
10001
11001
12001
13001

structural layering (Svekofennian orogenic fabric); T – ductile thrust shear zones; C' – extensional shear zones.

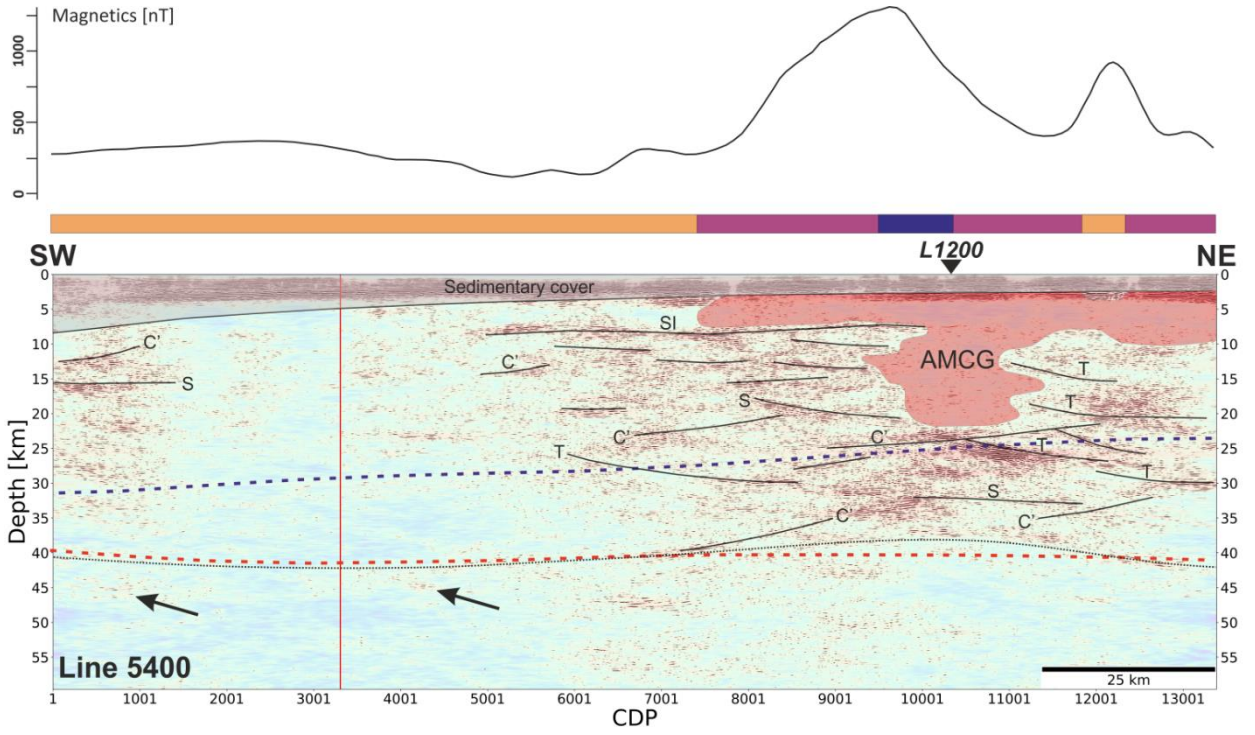

Figure 8: Final migrated depth-converted sections along PolandSPAN™ profile 5400 with its tentative interpretation. Bars atop the section are colour-coded according to the crystalline basement lithologies following Krzemińska et al. (2017) (see Fig. 9 for a legend). Magnetic profile at the top is extracted from the magnetic anomaly map (Fig. 3). S – subhorizontal structural layering (Svekofennian orogenic fabric); T – ductile thrust shear zones; C' – extensional shear zones.

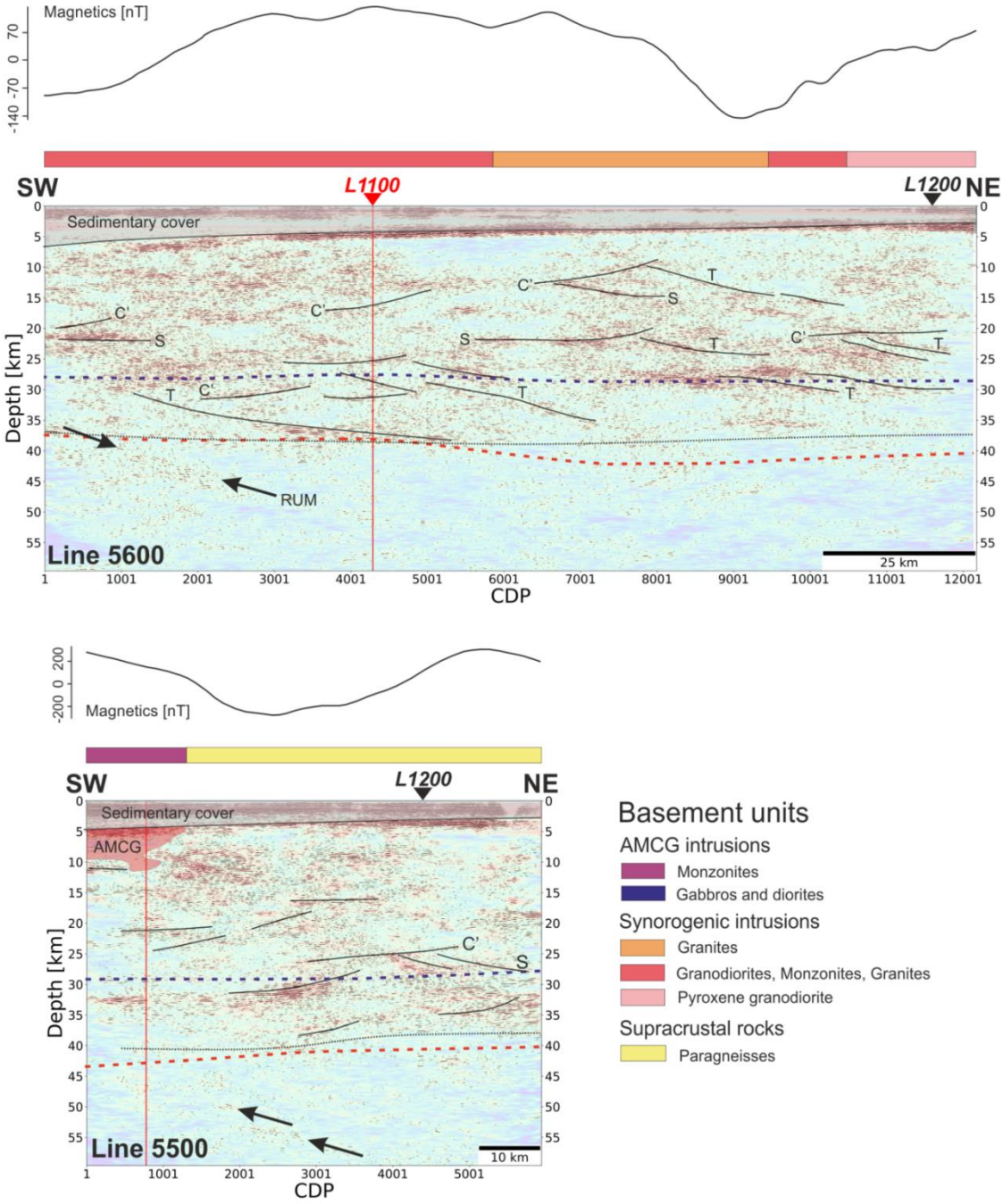

Figure 9: Final migrated depth-converted sections along PolandSPAN™ profiles ~~5600,~~ 5500 and ~~5400~~5600 with their tentative interpretation. Bars atop the section are colour-coded according to the crystalline basement lithologies following Krzemińska et al. (2017) (see Fig. 9 for a legend). Magnetic profile at the top is extracted from the magnetic anomaly map (Fig. 3). S – subhorizontal structural layering (Svekofennian orogenic fabric); T – ductile thrust shear zones; C' – extensional shear zones.

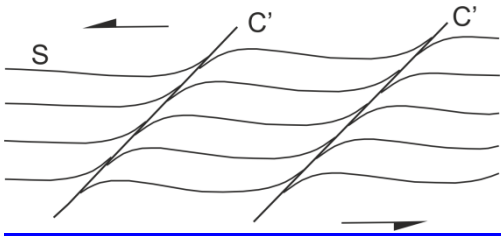

Figure 10: Schematic illustration of S-C' fabric. A set of extensional shear bands C' form oblique to the shear zone boundaries, dipping towards the shear direction in synthetic orientation. See also Fig. 16.22 in Fossen (2016).

1. Read uncorrelated SEG-D records
2. Extended correlation with ground force
3. Resample to 4 ms
4. Geometry setup and QC
5. Trace editing
6. Surface-consistent amplitude scaling (receivers and shots)
7. Spherical-divergence correction
8. Refraction statics (final datum 400 m.)
9. Minimum phase conversion
10. Surface-consistent deconvolution
11. Predictive deconvolution
12. Residual statics
13. FX Deconvolution
14. Bandpass filtering (2-6-38-48 Hz)
15. Residual statics
16. AGC
17. Kirchhoff DMO
18. CDP stack
19. Linear coherency filtering
20. Post-stack Stolt migration
21. Bandpass filtering (8-10-20-30 Hz)
22. Trace Equalization
23. Time-depth conversion

Table 1: Data processing scheme